Exotic 4-Manifolds Homotopy Equivalent to S^2

by

Tolga Temiz

A Dissertation Submitted to the
Graduate School of Sciences and Engineering
in Partial Fulfillment of the Requirements for
the Degree of

Master of Science

in

Mathematics

KOÇ ÜNİVERSİTESİ

June 20, 2023

Exotic 4-Manifolds Homotopy Equivalent to S^2

Koç University

Graduate School of Sciences and Engineering

This is to certify that I have examined this copy of a master's thesis by

Tolga Temiz

and have found that it is complete and satisfactory in all respects,
and that any and all revisions required by the final
examining committee have been made.

Committee Members:

_____

Prof. Dr. Burak ÖZBAĞCI (Advisor)

_____

Prof. Dr. Çağrı KARAKURT

_____

Prof. Dr. Sinan ÜNVER

Date: _____

To Emel CULBANT, Tuğçe TEMİZ CALAY, and Sürpriz TEMİZ

ABSTRACT

Exotic 4-Manifolds Homotopy Equivalent to S^2
Tolga Temiz
Master of Science in Mathematics
June 20, 2023

In this thesis, we will be reviewing morse theory and handle decompositions for manifolds while paying special attention to 4-manifolds and related notions such as handles moves and Kirby Calculus. We will also review the fundamentals of the relationship of knot theory and dimension four. The main objective will be to present an exotica result: There are exotic 4-manifolds with boundary that are homotopy equivalent to S^2, this result is due to Akbulut, [1]. I will not be presenting the original proof. Instead, we will be mainly following a different approach which is also present in [3]. In particular, I will be also following the lectures delivered by Piccirilo at *Tech Topology Summer School* and the lectures delivered at *Singularities and Low-Dimensional Topology Winter School, Alfred Renyi Institute of Mathematics.*

ÖZETÇE

S^2'ye Homotopik Eşdeğer Olan Egzotik 4-Manifoldlar
Tolga Temiz
Matematik, Yüksek Lisans
20 Haziran 2023

Bu tezde, manifoldlar için Morse teorisi ve kulp ayrışımları incelenecektir. 4-manifoldlara ve onlarla ilgili olan kulp hamleleri ve Kirby Kalkülüs gibi konulara ihtimam gösterilecektir. Ayrıca, düğüm teorisi ve dört boyutlu manifold teorisi arasındaki ilişkinin temel noktalarının da üzerinden geçilecektir. Asıl gayemiz, Akbulut tarafından bulunan bir egzotika sonucunu sunmaktır, [1] : S^2'ye homoptopik eşdeğer olan egzotik, sınırlı 4-manifoldlar vardır. Orijinal ispat sunulmayacaktır. Bunun yerine, büyük oranda [3]'de mevcut olan yaklaşım takip edilecektir. Spesifik olarak, Piccirillo tarafından *Tech Topology Summer School*'da verilen dersler ve *Singularities and Low-Dimensional Topology Winter School, Alfred Renyi Institute of Mathematic* dersleri takip edilecektir.

ACKNOWLEDGMENTS

I have been quite fortunate throughout my graduate education at Koç University as I had the opportunity to take many excellent courses at Koç University and Boğaziçi University delivered by Burak ÖZBAĞCI, Ferit ÖZTÜRK, and Umut VAROLGÜNEŞ. In addition to these, I was given the very valuable opportunities of attending *Georgia Tech. Topology Summer School*, where I attended the short course of Lisa Piccirillo; and *Singularities and Low-Dimensional Topology Winter School* at Alfred Renyi Institute of Mathematics. I would also like to thank my advisor Burak ÖZBAĞCI; Umut VAROLGÜNEŞ, and Kyle HAYDEN for many valuable discussions. Finally, I would like to thank my family and my friends, especially Dorukhan ÖZCAN for helping me in various ways constantly throughout my graduate education at Koç University, without whom this work would not have been possible.

TABLE OF CONTENTS

LIST OF FIGURES

ABBREVIATIONS

M	n-dimensional (smooth) manifold
(V, U, φ)	The chart $\varphi : V \to U$
D^k	k-dimensional ball (disk)
$\mathcal{A}$	A smooth atlas
TM	The tangent bundle of M
$Jac_p(f)$	The Jacobian of f at p
$Hess_f(p), Hess(f)$	The Hessian matrix of f at p
$ind_f(p)$	The index of a critical point p
$\nabla(f)$	The gradient of f
$d_pf, df(p)$	The differential of f at p
V^*	The dual space of the vector space V
D_p	The descending (unstable) manifold of p
A_p	The ascending (stable) manifold of p
$M(p, q)$	Flow lines from p to q
$M^*(p, q)$	The moduli space of flow lines from p to q
$c_i(f)$	Number of critical points of index i of f
$b_i(M)$	i-th Betti number of M
$\chi(M)$	The Euler characteristic of M
M_a^b	Denotes the set $f^{-1}([a, b])$
M^b	Denotes the set $f^{-1}([-\infty, b])$
S_a	The attaching sphere
S_b	The belt sphere
h^k	A k-handle
$w(K)$	The writhe of the knot K
Σ	A surface
$g(\Sigma)$	The genus of the surface Σ
$g_4(K)$	The slice genus of the knot K
$c_1(X)$	The first Chern class of X
T^2	The torus (i.e., $S^1 \times S^1$)
ν	Tubular neighborhoods

Chapter 1

INTRODUCTION

1.1 Exotic Structures

In 1950's, Milnor discovered the existence of some 7-dimensional smooth manifolds which are homeomorphic to S^7 but not diffeomorphic to it [12]. This was the first construction of an exotic smooth structure. It is known that there are no exotic smooth structures in dimensions 1,2 and 3. An interesting result regarding the Euclidean space $\mathbb{R}^n$ is the fact that there is a unique smooth structure unless $n = 4$ [17], in which case there are uncountably many exotic structures [6, 5, 19]. Investigation of smooth structures has been an active area of research. In particular, smooth generalized Poincaré conjecture in dimension 4 is one of the most motivating problems in low-dimensional topology at the moment: It is open whether the 4-sphere admits an exotic smooth structure.

1.1.1 Akbulut's Work

The result I will be rewieving in this thesis is a result of Akbulut [1]. This result demonstrates an exotic smooth structure on a 4-manifold with boundary which is homotopy equivalent to S^2. This manifold belongs to a family of manifolds, named knot traces. A knot trace, is a 4-manifold with boundary whose handle decomposition consists of a single 0-handle and a 2-handle. In particular, their Kirby diagrams are relatively simple, in the sense that, there is only a knot with a framing.

1.2 Resources

I have used many different resources for different purposes. I will now briefly mention about these. Firstly, Lee's *Introduction to Smooth Manifolds* is a standard textbook to begin with [10]. This book can be used for learning the basics of smooth manifolds. To learn Morse Theory, which yields the handle decompositions, I used mainly two textbooks: Milnor's *Morse Theory* and Matsumuto's *An Introduction to Morse Theory* [14, 11]. Milnor's book gives an interpretation in terms of the cellular decompositions and Matsumuto's book does the same for handle decompositions. I will refer to them while I am reviewing the Morse Theory and handle decompositions. Finally, a very comprehensive and excellent resource is *4-Manifolds and Kirby Calculus* by Gompf and Stipsicz [8]. The contents of this book cover the rest of the background material necessary to understand the main result of this thesis, so I will be referring to this textbook constantly. Finally, one last resource I would like to mention about is *Knots, Links, Braids and 3-Manifolds* by Prasolov and Sossinsly [16]. This book was very useful for me when I was trying to understand some notions such as framings and handle moves. However, this book is about 3-manifolds so we will not need it, but it is still a good resource for us especially for transitioning to the book of Gompf and Stipsicz.

1.3 Approach

As I mentioned in the abstract, I will first review Morse theory and handle calculus. Of course, I have to omit a huge deal of material but I will try to refer to the resources I mentioned before whenever necessary. Even though we are only interested in dimension 4, I will also very briefly talk about the general case as well as what happens in dimension 3 while I am reviewing handle decompositions and handle calculus. Once we complete our study of the background material, I will then talk about the main result, where I am going to give a more detailed discussion.

Chapter 2

PRELIMINARIES

2.1 Regarding This Chapter

In this chapter, I will first review some of the very fundamental notions such as the definition of a smooth manifold, then I will talk about Morse theory. This chapter is included for the completeness of the material. However, in the section 2.2, I will not review everything necessary to understand the rest of the material. For these topics, the reader is referred to [10].

2.2 Manifolds

Definition 1 *A topological space M is called a topological manifold of dimension n if for every $m \in M$, there exist an open subset of $U \in \mathbb{R}^n$, an open neighborhood of V of m, and a homeomorphism $\varphi : V \to U$. The triple (V, U, φ) is called a chart around m.*

Remark 1 *Being a topological manifold is a property. Sometimes, M is assumed to be Hausdorff and second countable as well. We will assume these when we are to define smooth manifolds.*

To be able to define a smooth structure, we need some compatibility condition on the charts. For this, let us define transition maps.

Definition 2 *Let M be a topological space, and $\varphi_1 : V_1 \to U_1$ and $\varphi_2 : V_2 \to U_2$ be coordinate charts. Then, the map $\varphi_2 \circ \varphi_1^{-1} : \varphi_1(V_1 \cap V_2) \to \varphi_2(V_1 \cap V_2)$ is called a transition map from (V_1, U_1, φ_1) to (V_2, U_2, φ_2).*

Remark 2 *The transition maps are automatically homeomorphisms. Moreover, they are maps from an open subset of $\mathbb{R}^n$ to another open subset of $\mathbb{R}^n$. Thus we can talk about differentiability of such maps. See figure 2.1.*

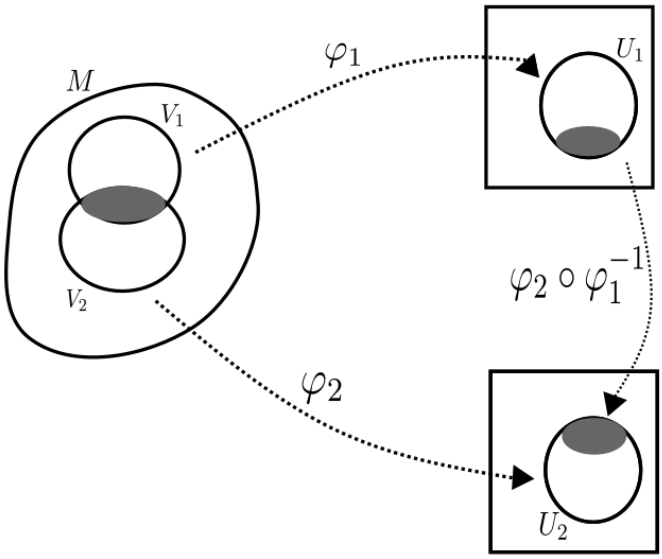

Figure 2.1: The transition map between (V_1, U_1, φ_1) and (V_2, U_2, φ_2), gray regions represent $V_1 \cap V_2$ and their images under the homeomorphisms.

Definition 3 *A smooth atlas on a topological space M is a collection of charts $\{\varphi_i : V_i \to U_i\}_{i \in I}$ such that*

- $\bigcup V_i = M$,
- *All transition maps between any two charts in the collection I are smooth.*

Definition 4 *A smooth atlas $\mathcal{A}$ is called maximal if any chart that has smooth transition maps to all the charts in $\mathcal{A}$ is already in $\mathcal{A}$.*

Definition 5 *A smooth manifold is a second countable and Hausdorff topological space that is equipped with a maximal smooth atlas.*

Remark 3 *A maximal smooth atlas is called a smooth structure. It is important to realize that a smooth structure is an additional piece of data. It is not a property of the topological space. This is why it makes sense to talk about exotic structures, as the main result of this thesis will demonstrate.*

Example 1 *The real line $\mathbb{R}$ as a topological space can be equipped with the following two charts: $id_{\mathbb{R}} : \mathbb{R} \to \mathbb{R}$ and $x \mapsto x^3$. They are both homeomorphism. Since each smooth atlas is contained in a unique maximal smooth atlas*[1]*, we have two smooth structures. Moreover, the transition map between these two charts is given by $x \mapsto \sqrt[3]{x}$, which is not differentiable at $x = 0$. Hence, these smooth structures are distinct. However, they are not essentially different. We can make this precise by the following definition.*

Definition 6 *Let M_1 and M_2 be two smooth manifolds. A smooth map that is also a bijection $f : M_1 \to M_2$ is called a diffeomorphism if its inverse is also smooth. Furthermore, M_1 and M_2 are called diffeomorphic if there is a diffeomorphism between them.*

Remark 4 *We would like to consider smooth manifolds up to diffeomorphisms. So, when we say that we have an exotic smooth structure, what is meant is a pair of homeomorphic manifolds that are not diffeomorphic. In particular, what we mean is not two distinct smooth structures as in example 1. Indeed, as expected*[2]*, the smooth manifolds in example 1 are diffeomorphic.*

Now, in the Morse Theory section, we will need the definition of the tangent space (at a point in M). Let us define the tangent bundle and the tangent space as well. Given open subsets $U \subset \mathbb{R}^n$ and $V \subset \mathbb{R}^m$ and a smooth map $f : U \to V$. Let's first define the tangent bundle as $TU = U \times \mathbb{R}^n$, which is an open subset of $\mathbb{R}^{2n}$. We can also define the differential map:

$$df : TU \to TV,$$

by $df(p, v) = (f(p), Jac_p(f)v)$, where $Jac_p(f)$ denotes the Jacobian matrix of f at p.

Definition 7 *For a smooth manifold M with a maximal smooth atlas $\{\varphi_\alpha : V_\alpha \to U_\alpha\}_{\alpha \in I}$, set $U_{\alpha\beta} = \varphi_\alpha(V_\alpha \cap V_\beta)$. We define TM by gluing TU_α along $TU_{\alpha\beta} \subset TU_\alpha$ using $d(\varphi_\beta \circ \varphi_\alpha^{-1})$.*

[1] See [10], Proposition 1.17.

[2] As mentioned in chapter 1 there are no exotic smooth structures in dimensions 1,2, and 3.

Now, given a smooth map $f : X \to Y$, then there is a canonical smooth map $df : TX \to TY$. We also have $\pi : TM \to M$ by $(p, v) \mapsto \varphi_\alpha^{-1}(p)$.

Definition 8 *For $p \in M$, $\pi^{-1}(p)$ is called the tangent space of p is denoted by T_pM.*

We also need to define transversality for the Morse Theory section.

Definition 9 *Given a smooth manifold M and two submanifold Z and N, Z and N intersect transversaly if*

$$T_pN + T_pZ = T_pM, p \in M,$$

and denoted by $Z \pitchfork N$.

A consequence of transversality is that, if $Z \pitchfork N$, then $Z \cap N$ is a submanifold as well.

2.3 Morse Theory and Cell Decompositions

Definition 10 *Given a smooth function $f : M \to \mathbb{R}$, and $p \in M$. The point p is called a critical point if $df_p = 0$, and it is called nondegenerate if in some local coordinate $(x_1, \cdots, x_n)$ (such that the origin is p) the Hessian defined by $Hess_f(p) = (\frac{\partial^2}{\partial x_i \partial x_j}|_0)_{i,j=1,\cdots,n}$ is nondegenerate. If all critical points of f are nondegenerate, then f is called Morse.*

Remark 5 *The above definition is well-defined, meaning that the nondegeneracy of the Hessian matrix is independent of the choice of the local coordinates. For a proof of this, see [14], chapter 1.*

Theorem 1 (Morse Lemma) *Let $f : M \to \mathbb{R}$ be a Morse function, and suppose $p \in M$ is a critical point. Then there exists local coordinates $(x_1, \cdots, x_n)$ such that*

$$f(x) = f(p) - (x_1^2 + \cdots + x_k^2) + (x_{k+1}^2 + \cdots + x_n^2)$$

The number k is called the index of the critical point p and is denoted by $ind_f(p)$.

Proof *A complete proof of this can be found in [14]. Here is a slightly different approach for the case $n = 1$ (in fact, this can also be extended to a complete proof by induction, see [4]): Suppose, by passing to local coordinates, that $f : \mathbb{R} \to \mathbb{R}$ is a Morse function with a critical point at $x = 0$. By using Taylor's Theorem with integral remainder, we have*

$$f(x) = f(0) + \frac{1}{2}f''(0)x^2 + \varepsilon(x)x^2 = f(0) \pm ax^2(1 + \tilde{\varepsilon}(x)),$$

where a is a positive real number and $\varepsilon(x) = \frac{1}{2}\int_0^x f^{(3)}(t)(x-t)^2 dt$. We let $x_1 = \varphi(x) = x\sqrt{a(1+\tilde{\epsilon}(x))}$. Since φ is a local diffeomorphism, by the Inverse Function Theorem, $f \circ \varphi^{-1}(x_1) = f(x) = f(0) \pm x_1^2$, as desired.

Remark 6

- *The charts in the Morse Lemma are called Morse charts.*
- *Morse Lemma is equivalent to the fact that the Hessian can be diagonalized in such a manner that all the entries along the diagonal are ± 2.*
- *The index of a critical point does not depend on the particular choice of such local coordinates because Hessians corresponding to different local coordinates are congruent (by the Jacobian matrix of the change of coordinates), symmetric, and real matrices, by Slyvester's Law of Inertia, the number of positive and negative eigenvalues they possess are the same and the index is precisely the number of negative eigenvalues.*
- *Morse Lemma implies that critical points of a Morse function are isolated (this can be seen by doing the computations in a Morse chart).*
- *On a compact manifold, a morse function can only have finitely many critical points, this follows from the previous item.*

Theorem 2 *On a compact manifold M, the set of Morse functions on M is a dense open subset of $C^\infty(M;\mathbb{R})$.*

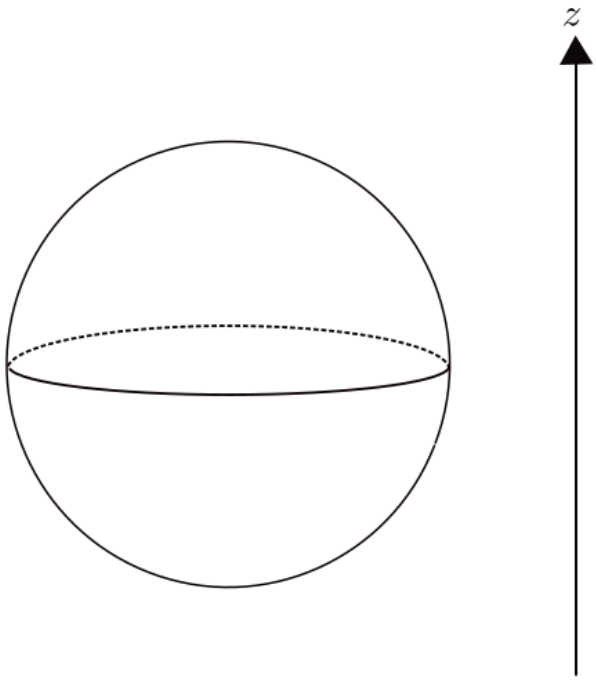

Figure 2.2: The height function on S^2 is a Morse function.

Remark 7 *This theorem tells us that Morse functions are not rare. For a proof, see [4].*

Example 2 *The height function on S^2 with respect to the z coordinate is a Morse function, see figure 2.2. In the upper hemisphere, $f(x, y) = \sqrt{1 - x^2 - y^2}$. It can be directly computed using this local coordinates that f is Morse with the critical point $(0, 0, 1)$. Similarly, it also has $(0, 0, -1)$ as a critical point. Their indices are 2 and 0, respectively.*

Remark 8 *In the previous example, the indices can also be interpreted as follows: At the point $(0, 0, 1)$, f attains its maximum value, therefore, there should be no increasing directions, thus, we expect to see $f(x, y) = 1-x^2-y^2$ in a Morse chart, hence its index must be 2. A similar interpretation can be made for the point $(0, 0, -1)$. Moreover, around a Morse chart at a maximum, we have a cap-like shape while*

around a minimum, we have a bowl-like shape. Note also that on a compact manifold, there is always a maximum and minimum, thus any Morse function necessarily yields these two shapes at least once. Regarding critical points of index 1*, in local coordinates, it should look like a saddle. The next example will provide us with such a critical point as well.*

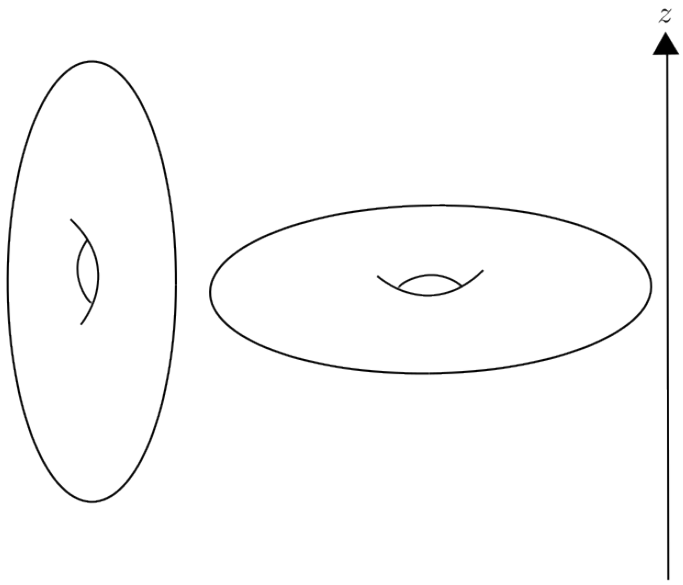

Figure 2.3: Two height functions on $S^1 \times S^1$.

Example 3 *In this example, we consider two height functions on the torus, see figure 2.3. The one on the right is not a Morse function since it has infinitely many critical points. The one on the left is a Morse function, similar to the sphere example this one also has critical points of indices* 0 *and* 2*. In addition to these, the points placed in the upper and lower end points of the arcs in the middle are also critical points. These are critical points of index* 1*, and as expected, each has two direction*

along one of which the morse function is increasing and along the other, the morse function is decreasing.

Given a Morse function on a compact manifold, we can track the level sets together with everything that lies below the level set. For instance, in both examples, this set is empty until we look at the global minimum, at which this set is just a point. Then, until we reach at the next critical point, we have a bowl-like shape, whose homotopy type is again a point. It can be seen that at each critical point, the homotopy type changes. We can use a Morse function to keep track of this change in the homotopy type as we increase the values. This is a useful approach that yields a cellular decomposition of a compact manifold. Let us take a look at the following example.

Example 4 *As seen in the previous example, $S^1 \times S^1$ has 4 critical points. We can keep track of the change in the homotopy type by considering a cellular decomposition. Passing each of these critical points is equivalent to attaching a cell (D^k), where k is the index of that critical point. Looking at figure 2.4, when we are at the minimum a point appears. Then passing this point introduces a bowl-like shape, which has the homotopy-type of a 0-dimensional disk (they are the same), i.e. a 0-dimensional cell. Passing the first critical point of index 1 is equivalent to attaching a 1-cell, i.e. a closed interval. The third picture corresponds to the moment we pass the second critical point of index 1, and it is equivalent to attaching a 1-cell again. Finally, the maximum point, which is a critical point of index 2, correspond to attaching a 2-cell, which is the closed disk in $\mathbb{R}^2$.*

Remark 9 *One can think of cells as the decreasing directions at a critical point (to be precise, it can be related to the descending manifold of that critical point, we will talk about this notion in the Morse Homology section). We will not be working with cellular decompositions because we are going to be interested in the diffeomorphism-type of the resulting manifold at each step. This can be achieved by considering handle decompositions, which we will talk about later. For more information on cellular decompositions, see [14].*

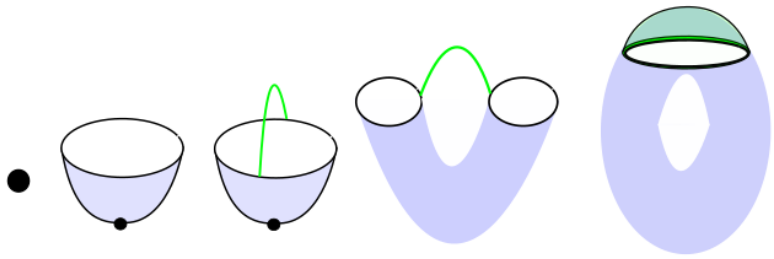

Figure 2.4: Cellular decomposition of $S^1 \times S^1$.

2.4 Morse Homology

This section is not necessarily needed for the rest of the work but it is a different approach to Morse theory, and for completeness, I will briefly summarize Morse Homology and its results. It is also practical to have this picture in mind when considering handle decompositions. Moreover, Morse Homology can be used to prove the Morse Inequalities, which themselves yield interesting observations regarding handle decompositions. I will omit some of the proofs or some details of them, see, for instance, [4] for the details. Let M^n be a smooth closed manifold, $f : M \to \mathbb{R}$ be Morse, and g be a Riemannian metric on M (a smoothly varying positive-definite inner product on $T_p(M), \forall p \in M$).

Definition 11 *The gradient ∇f of f is defined by $g(\nabla_p f, v) = d_p f(v), v \in T_p(M)$.*

Remark 10 *This definition makes sense because g induces a nondegenerate pairing $T_p(M) \times T_p(M) \to \mathbb{R}$, hence an isomorphism $T_p(M) \simeq T_p^*(M)$, where $*$ denotes the dual space. Since $d_p f \in T_p^*(M)$, by the isomorphism just described, there has to be a vector in $T_p(M)$, whose image is $d_p f$, we call this $\nabla_p f$. In other words, the gradient is the g-dual of $d_p f$.*

Before introducing the necessary tools to develop the Morse Homology, we can have the following intuition in mind: Consider a surface made out of glass and a liquid

on it which moves under the effect of gravity only, and this liquid never leaves the surface. Then, we can keep track of the movement of the drops. It can be seen that every drop necessarily goes to a critical point and if we turn the time back we can imagine it coming from a critical point as well. This, gives us a way to connect critical points. In particular, the complex will be the free abelian groups generated by the set of critical points (sorted according to the index), and the boundary maps will essentialy count the flow lines of such drops.

With this interpretation and the height function examples in mind, it makes sense to consider the negative gradient flow. The negative gradient $-\nabla f$ is a vector field, it has a flow $\varphi_t : M \to M$, note that this vector field is complete since M is closed. This flow then satisfies the following:

$$\frac{\partial}{\partial t}\varphi_t(p) = -\nabla_p f.$$

If p is a critical point, then $d_p f = 0$, which implies that $-\nabla_p(f) = 0$ by definition and hence $\frac{\partial}{\partial t}\varphi_t(p) = 0$, thus the critical points are precisely the stable points of this flow. Moreover, if p is not critical, then $\frac{\partial}{\partial t} f(\varphi_t(p)) = \nabla f_p \cdot \frac{\partial}{\partial t}\varphi_t(p) = -||\nabla f_p|| < 0$, implying that the values are strictly increasing under this flow for regular points.

Remark 11 *I decided to use the negative gradient flow to match with the intuition I provided at the beginning of this section but everything works perfectly fine if one chooses to work with the gradient flow itself. The difference will be that the flow is moving upward and instead of Morse Homology, one obtains Morse Cohomology.*

Definition 12 *For a nondegenerate critical point p of index k, we define the following two manifolds:*

$$D_p = \{x \in M : \lim_{t\to-\infty} \varphi_t(x) = p\},$$

$$A_p = \{x \in M : \lim_{t\to\infty} \varphi_t(x) = p\}.$$

These are named the descending and the ascending manifold of p, respectively, and they are manifolds. In fact, they are diffeomorphic to disks of dimension k and $n-k$ respectively. Moreover, T_pD_p and T_pA_p are negative and positive eigenspaces of $Hess(f)$, respectively.

Remark 12 *Descending and ascending manifolds are also called unstable and stable manifolds.*

Remark 13 *Note that, because M is closed (hence compact), every point in M belongs to precisely one descending manifold and one ascending manifold. This is true since, for instance, as t goes to infinity, noncritical points strictly decrease and their values cannot escape to negative infinity. The rate of decrease cannot get smaller indefinitely as this would mean we are approaching to a critical point since stable points are precisely the critical points. Hence, indeed, every point in M belongs to a unique descending (ascending) manifold. Intuitively, every point flows from one critical to another.*

Let us try to understand these concepts by considering the following two examples.

Example 5 *In this example, we will consider the case of S^2. In figure 2.5 we see some of the flow lines. Let's consider the maximum, denoted by a blue star, the stable manifold of this point consists of only itself, since every other orbit decreases strictly and necessarily goes to the minimum point. This is consistent with the information given in the definition since the maximum is a critical point of index 2 and its stable manifold is a $2-2=0$-dimensional disk, i.e. a point. The unstable manifold of this point is the whole S^2 except for the minimum, which is diffeomorphic to a disk of dimension 2, as expected. A similar analysis can be made for the minimum, red star, as well.*

Example 6 *Now, let's consider the torus. In figure 2.6, we can see some of the flow lines. The blue star, is a maximum and similar to the previous example, its unstable manifold is a 2-disk. Similarly, for the yellow star as well. The stable manifold of the green star consists of all the points on the two flow lines from the blue star to the green one and the green star itself. Therefore, it is just an interval as expected. Its unstable manifold also consists only of the green flow lines and itself, so again an interval. The phenomenon that will be useful is to notice the following: There*

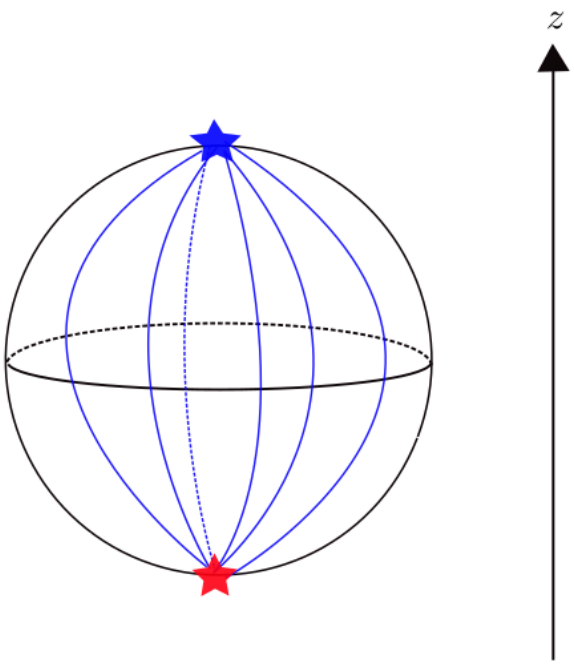

Figure 2.5: Flow lines in S^2.

are only two flow lines from the red star to the yellow star (similarly from the blue star to the green one). This is true in general, if the index difference between two critical points is 1*, then the number of flow lines between them is finite.*

Remark 14 *Regarding the fact T_pD_p and T_pA_p are negative and positive eigenspaces of $Hess(f)$, respectively, we can see this as follows: Around a critical point p, by Morse Lemma, $f(x_1, \cdots, x_n) = f(p) - (x_1^2 + \cdots + x_k^2) + (x_{k+1}^2 + \cdots + x_n^2)$. Restricting this function to $\{x_{k+1} = \cdots = x_n = 0\}$, we have $f(x) = f(p) - (x_1^2 \cdots + x_k^2)$. Then T_pD_p is spanned by vectors*

$$(1, 0, \cdots, 0), (0, 1, 0, \cdots, 0), \cdots, (0, 0, \cdots, 1, 0, \cdots, 0).$$

These are precisely the eigenvectors of $Hess(f)$ whose eigenvalues are -2 (recall that Hessian in a Morse chart is a diagonal matrix consisting of -2's and 2's). Thus,

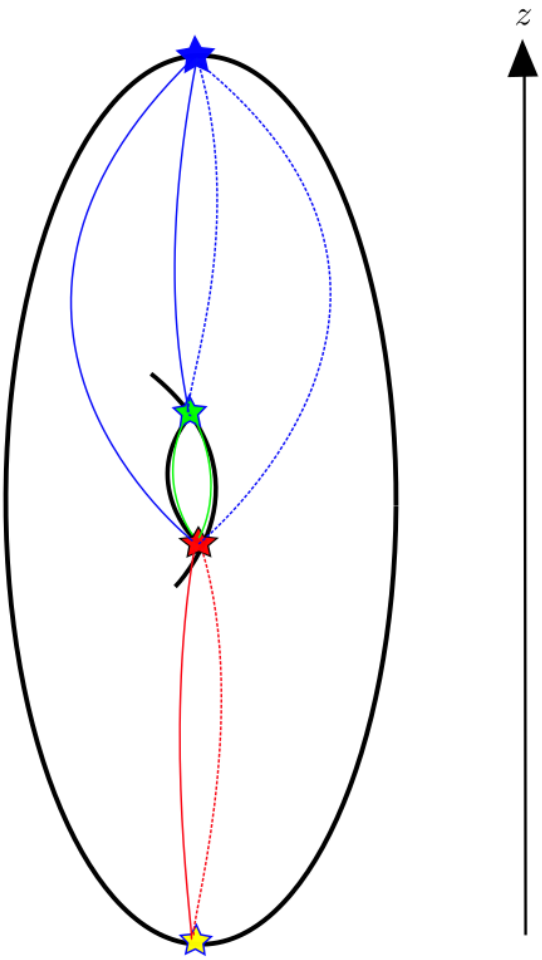

Figure 2.6: Flow lines in $S^1 \times S^1$.

negative eigenspace of $Hess(f)$ *is* T_pD_p. *The argument is similar for* T_pA_p.

Now, in order to be able to count these flow lines, we need to intersect stable and unstable manifolds, and we want the intersection to be a submanifold as well. We know that transverse intersection of submanifolds is again a submanifold. Thus, we need the transversality condition.

Definition 13 *The tuple* (f, g) *is called Morse-Smale if for any* $p, q \in M$, $A_p \pitchfork D_q$. *In this case, we define* $M(p, q) = A_p \cap D_q$.

Remark 15 *Putting the Morse-Smale condition does not restrict the Morse functions because for a generic choice of the Riemannian metric g, (f, g) is Morse-Smale.*

Remark 16 *By counting the dimensions, we can see that $M(p, q)$ is a manifold of dimension $ind(p) - ind(q)$. This also implies that if $ind(p) \leq ind(q)$, then $M(p, q) = \emptyset$ (since $M(p, q)$ has to be at least 1-dimensional as it has to contain all the points on a given flow line).*

Definition 14 *By declaring $\varphi_t(x) = \varphi_{t'}(x)$, we can define the moduli space of flow lines between p and q, denoted by $M^*(p, q) \simeq M(p, q)/\mathbb{R}$. The dimension of $M^*(p, q)$ is equal to $dim(M(p, q)) - 1 = ind(p) - ind(q) - 1$.*

Remark 17 *$M^*(p, q)$ can be thought of as $f^{-1}(c) \cap M(p, q)$ for any regular value c between p and q. Note that $M^*(p, q)$ is compact for the sphere example as it is just S^1, where p and q denote the maximum and the minimum, respectively. This is not always the case. Nevertheless, $M^*(p, q)$ can be compactified by adding broken flow lines. I will make a small argument for this.*

Example 7 *Consider $S^1 \times S^1$, see 2.6, it is not Morse-Smale since $M(p, q) \neq \emptyset$, where p and q are the index 1 critical points (there are green flow lines between them). This can be overcome by perturbing the Torus. In the following example, we will consider such a Torus.*

Example 8 *Now, we will consider the perturbed torus, see figure 2.7. In the sphere example, if we pick, say 0, level set, then $M^*(p, q) = f^{-1}(c) \cap M(p, q) \simeq S^1$, and therefore it is compact. However, the same argument does not work here and is instructive to try the same. Say we pick a value close to the maximum, then $M^*(p, q)$, where p is the maximum and q is the minimum, is no longer compact because not all the flow lines are from p to q, there are some flow lines from p to index 1 critical points as well. This suggests that we need to add some broken flow lines. This can be seen better from the figure on the right-hand side of 2.7. Let's focus our attention to the bottom right square. Here, the flow lines from the blue star to the yellow star are approaching to the union of the sides of this bottom right square, which is precisely*

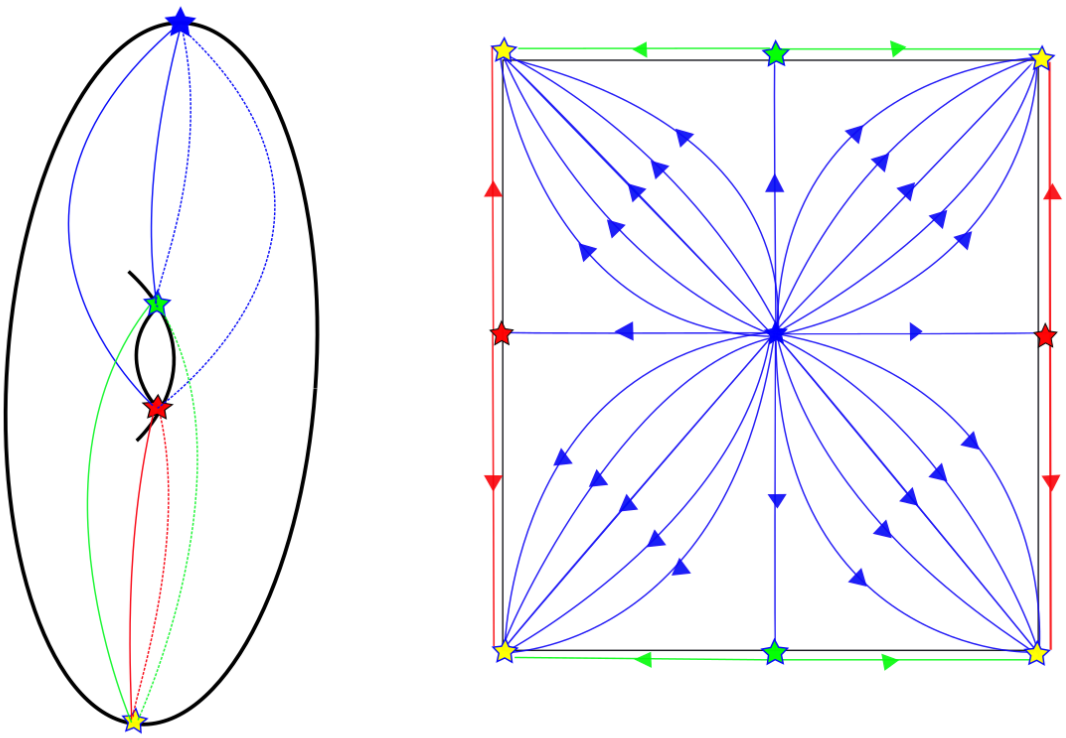

Figure 2.7: Compactification of the moduli space of $S^1 \times S^1$.

the broken flow line first following the blue and then the red (or green). If we add this limiting case, we will have a compact space, this will be the compactification of the moduli space.

Now, let's talk about the formulation of this compactification. The compactification is also important as it plays a role in the proof of the fact that the boundary map in the Morse Homology is a differential.

Theorem 3 *Let M be a closed manifold, and (f, g) be Morse-Smale. Then $M^*(p, q)$ has a natural compactification for $ind(p) > ind(q)$:*

$$\overline{M^*}(p,q) = \bigcup_{k=0}^{ind(p)-ind(q)-1} \bigcup_{r_i \in Crit(f)} M^*(p, r_1) \times M^*(r_1, r_2) \times \cdots \times M^*(r_k, q),$$

$\overline{M^*}(p, q)$ is a smooth manifold with corners.

If the index difference of p and q is equal to 1, then since there are no intermediate critical points to form broken flow lines, $M^*(p,q)$ is compact. Moreover, its dimension is $ind(p) - ind(q) - 1 = 0$. If the index difference is equal to 2, then $\partial\overline{M^*}(p,q) = \bigcup_{ind(r)=ind(q)+1} M^*(p,r) \times M^*(r,q)$, this is the boundary of a compact 1-dimensional manifold, i.e. the boundary of a union of closed intervals, its cardinality is even and this will be useful as we will see now.

Definition 15 *Suppose (f,g) is Morse-Smale on a smooth closed manifold M. Define $C_k^M(f,g) = \bigoplus_{ind(p)=k} p\mathbb{Z}_2$, i.e. the $\mathbb{Z}_2$ vector space generated by $\{p : ind(p) = k\}$. We also define $\partial_k^M p = \sum_{ind(q)=k-1} |M^*(p,q)|q \in C_{k-1}^M(f,g)$.*

Lemma 1 $\partial^2 = 0$.

Proof *Let $ind(p) = k$. Then $\partial^2 p$ is equal to:*

$$\partial\Big(\sum_{ind(r)=k-1} |M^*(p,r)|r\Big) = \sum_{ind(q)=k-2} \sum_{ind(r)=k-1} |M^*(p,r)||M^*(r,q)|q.$$

The coefficient of a fixed q is equal to $\sum_{ind(r)=k-1} |M^*(p,r)||M^*(r,q)| = |\partial M^*(p,q)| = 0$, since we are working over $\mathbb{Z}_2$.

By the above lemma,

$$C^M(f,g) = \cdots \xrightarrow{\partial_{k+1}} C_k(f,g) \xrightarrow{\partial_k} \cdots$$

is a chain complex. The homology of this chain complex is called the Morse Homology of (M,f,g).

Remark 18 *One can also work over $\mathbb{Z}$, in that case one needs to take orientations into consideration as well.*

Theorem 4 *Let M be a closed smooth manifold and (f,g) be Morse-Smale. Then*

$$H_*(f,g) \simeq H_*(M).$$

This theorem tells us that our choices of the morse function f and the Riemannian metric g does not make a difference in the homology. We will use this theorem to prove Morse inequalities. Before doing that, let us compute the Morse Homology of the sphere.

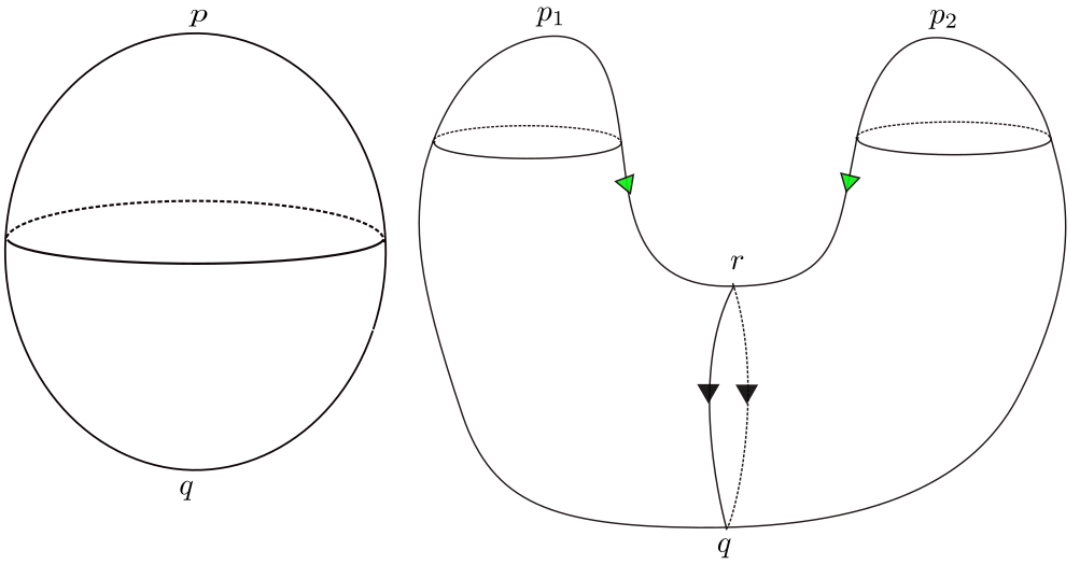

Figure 2.8: Two S^2's.

Example 9 *In this example, we will compute the Morse Homology of* S^2*, we will do this twice, for both surfaces in figure 2.8, which are both diffeomorphic to* S^2*. Focusing on the figure on the left, the complex has the form:*

$$\cdots 0 \xrightarrow{\partial_3} C_2(M) \xrightarrow{\partial_2} C_1(M) \xrightarrow{\partial_1} C_0(M) \to 0 \to \cdots .$$

Since there are no critical points of index 1*, the middle vector space is the* 0 *space. Thus all the maps are zero maps, hence* $H_0(f,g) = \langle q \rangle \simeq H_2(f,g) = \langle p \rangle \simeq \mathbb{Z}_2$*, and* $H_1(f,g) = 0$*. This was expected since the Morse Homology is isomorphic to the singular homology. The figure on the right is more interesting. In this case* $C_2(M) = \langle p_1, p_2 \rangle, C_1 = \langle r \rangle$*, and* $C_0(M) = \langle q \rangle$*. Note that* $\partial_1(r) = 2q$ *(there are two flow lines from* r *to* q*). We are working over* $\mathbb{Z}_2$*, so* $\partial_1 = 0$*. Also, note that* $\partial_2(p_1) = \partial(p_2) = r$*. The complex takes the following form:*

$$\cdots 0 \xrightarrow{\partial_3} C_2(M) \xrightarrow{\partial_2} C_1(M) \xrightarrow{0} C_0(M) \to 0 \to \cdots .$$

Thus $H_0(f,g) \simeq \mathbb{Z}_2$*, and* $H_1(f,g) = 0$ *(both the kernel and the image are* $\langle r \rangle$*). Moreover,* $H_2(f,g) = ker(\partial_2) = \langle p_1 - p_2 \rangle \simeq \mathbb{Z}_2$*, as expected.*

Now, we are ready to talk about Morse Inequalities.

Theorem 5 *Let $c_i(f)$ denote the number of critical points of f of index i, $b_i(M)$ denote the i-th Betti number of M, i.e. the rank of the i-th homology of M, and $\chi(M)$ denote the Euler characteristic of M. Then*

$$\sum_{i=0}^{k}(-1)^{k-i}c_i(f) \geq \sum_{i=0}^{k}(-1)^{k-i}b_i(M),$$
$$c_k(f) \geq b_k(M),$$
$$\sum_{i=0}^{n} c_k(f) = \chi(M).$$

Proof *Since*

$$c_k(f) = dim(ker(\partial_k)) + dim(im(\partial_k)),$$

and

$$dim(im(\partial_k)) - dim(ker(\partial_{k-1})) = -b_{k-1}(M),$$

expanding the left-hand side of the first expression and adding $-rank(im(\partial_{k+1}))$ yield the first inequality. If we are on the top level, then $\partial_{n+1} = 0$, thus the inequality turns into an equality and this proves the third one. The second one can be seen by direct comparison.

Remark 19 *These inequalities connect the number of critical points of a Morse function to the topology of the manifold. For instance, the second inequality tells us that on the torus, there does not exist a Morse function with total number of critical points less than 4. This also tells us something about the handle decompositions as well, there is no handle decomposition of torus with less than 4 handles.*

Remark 20 *As noted before, it is good to have a picture of Morse Homology, at least the ascending and descending manifolds in mind when working with handles. Morse inequalities are also important results in morse theory. Nevertheless, Morse homology is not needed for proving the morse inequalities, see [14] for a proof without developing the Morse Homology.*

Chapter 3

HANDLES, HANDLE DECOMPOSITIONS

From this chapter on, almost all the details I will be skipping can be found in [8]. For some Morse theory related details and more, the reader can also refer to [13]. Another good resource is [11], which is quite accessible.

3.1 Handles

Given a Morse function $f : M \to \mathbb{R}$, where M^n is a smooth manifold. For $[a, b] \subset \mathbb{R}$, let $M_a^b = f^{-1}([a, b])$, and $M^b = f^{-1}((-\infty, b])$. If there exists a unique critical point between a and b, say of index k, then from the previous chapter:

$$M^b \simeq M^a \cup D^k,$$

where $\simeq$ denotes homotopy equivalence. The idea in this chapter will be to replace D^k with $D^k \times D^{n-k}$, the latter can be considered as a thickened up k-cell. In this case, we will have

$$M^b \simeq M^a \cup D^k \times D^{n-k},$$

where $\simeq$ denotes diffeomorphic. To be able to talk about such objects, we will need some terminology.

Definition 16 *An n-dimensional k-handle is $h^k = D^k \times D^{n-k}$. See figure 3.1 for a 3-dimensional $1-$handle.*

Definition 17 *Given h^k as above: $D^k \times \{0\}$ is called the core, and $\{0\} \times D^{n-k}$ the co-core; $S^{k-1} \times \{0\} = S_a$ is called the attaching sphere, and $\{0\} \times S^{n-k-1} = S_b$ the belt sphere; $S^{k-1} \times D^{n-k}$ is called the attaching region, and $D^k \times S^{n-k-1}$ the belt region. See figure 3.2. In this figure, in the picture on top, the green region is the attaching region, the blue region is the attaching sphere, the green line segment is*

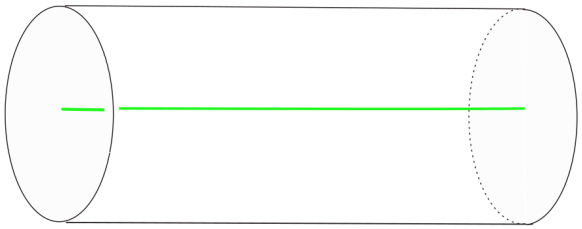

Figure 3.1: 3-dimensional 1-handle.

the core; in the picture below, the yellow region is the co-core, the pink boundary is the belt sphere.

Note also that $\partial(h^k) = S^{k-1} \times D^{n-k} \bigcup D^k \times S^{n-k-1}$, i.e., the boundary is the union of the attaching region and the belt region. Now, the following theorem is the main result, after stating the result I will clarify some of the details.

Theorem 6 *Suppose that there is only one critical point in $f^{-1}([a,b])$. Let k be the index of this critical point, then*

$$M^b \simeq M^a \cup_\varphi h^k,$$

where the k-handle is attached along a map $\varphi : S^{k-1} \times D^{n-k} \to \partial M^a$. Here $\simeq$ denotes a diffeomorphism.

Remark 21 *$M^a \cup_\varphi h^k$ is, in fact, a manifold with corners but there is canonical way of smoothing out the corners, we consider the corresponding smooth manifold.*

Now, we can have an understanding of this theorem if we view the critical point from above. We shall consider the figure 3.3. This is the picture of a critical point. Working in a Morse Chart, and assuming the critical value is 0, f has the following form $f(x,y) = |y|^2 - |x^2|$, where $x = (x_1, \cdots, x_k)$ and $y = (y_1, \cdots, y_{n-k})$. As noted in the Morse theory chapter, the decreasing directions give us a cell, in this picture

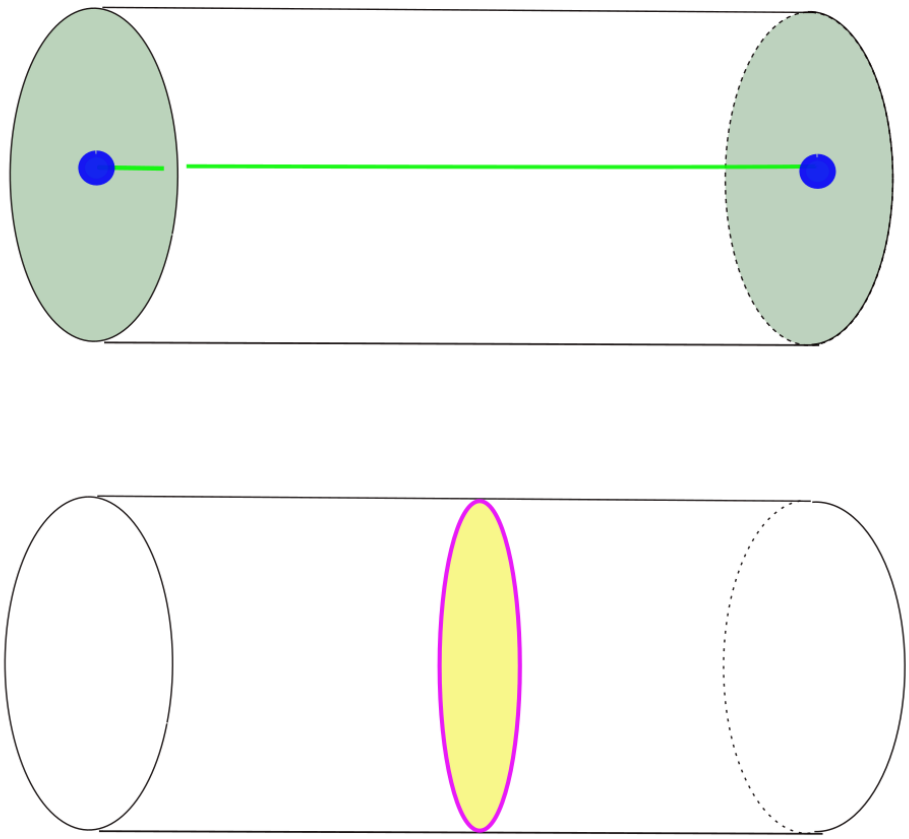

Figure 3.2: Anatomy of a handle.

this is the line segment denoted by the darker green color and it is attached to the boundary of M^a as can be seen from the figure. Now we thicken this cell up and smooth it, we obtain the green region, which corresponds to our handle.

Remark 22 *We can also see the connection to the flow lines of f. We shall consider figure 3.4. We do know that the core is actually the cell from the cellular decomposition, it represents the decreasing directions, thus the core of h^k is equal to $D_p \cap h^k$. Moreover, the co-core of h^k corresponds to directions that are increasing,*

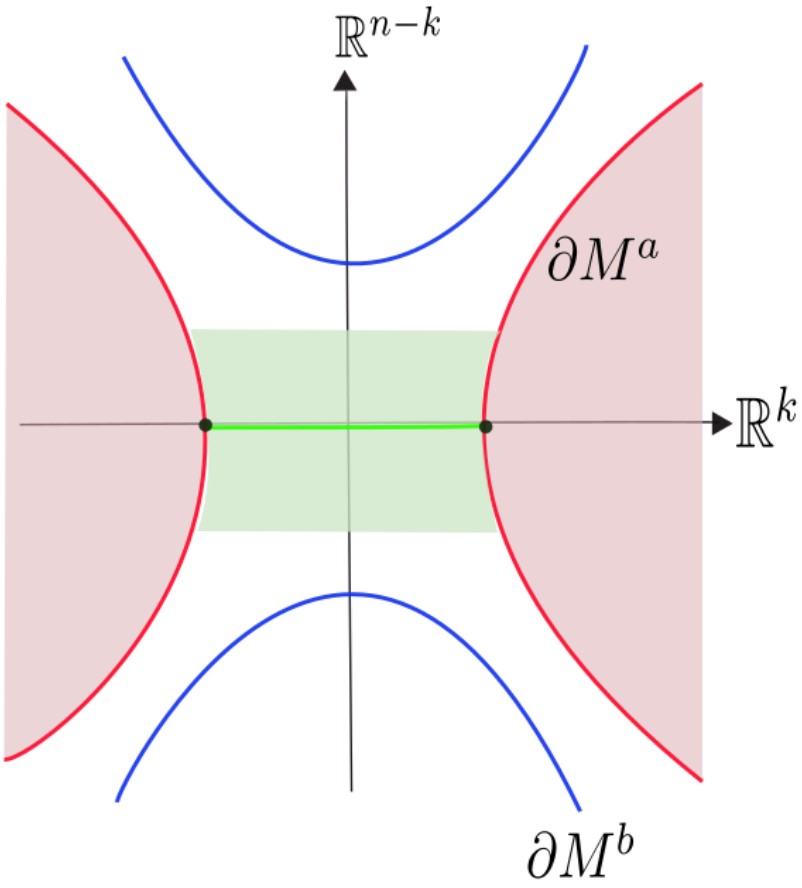

Figure 3.3: A critical point from above.

under the negative gradient flow, these corresponds to directions we can approach to our critical point, thus it is equal to $A_p \cap h^k$.

The next theorem will help us classify all possible attachments of a handle. Using this theorem, we are going to focus on the cases of low-dimensional manifolds in the following chapters.

Theorem 7 *The map* $\varphi : S^{k-1} \times D^{n-k} \to \partial M^a$ *is completely determined up to isotopy by:*

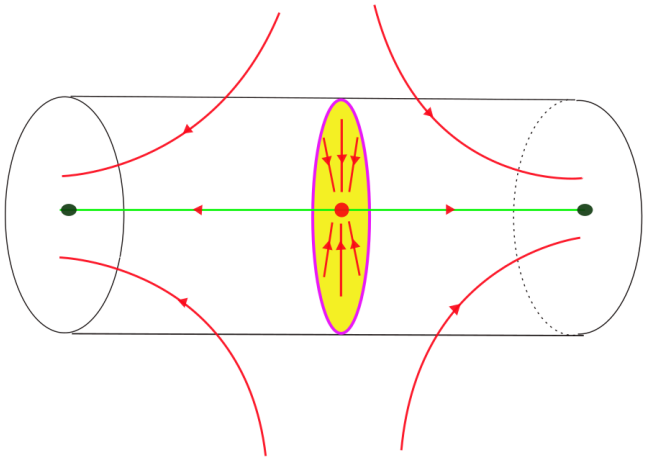

Figure 3.4: A handle and flow lines of f.

- $\varphi|_{S_a} : S^{k-1} \times 0 \to \partial M^a$,
- *a framing of* $\varphi(S_a)$, *i.e.,* $\nu(\varphi(S_a)) \simeq \varphi(S_a) \times D^{n-k}$.

Remark 23 *We first attach the core, and then thicken it up, but while thickening up we can twist it as well. We need to specify a tubular neighborhood of* $\varphi(S_a)$, *for this we need to specify an orthonormal basis for* D^{n-k} *at each* $p \in S^{k-1}$, *i.e., we need need to specify a map* $S^{k-1} \to O(n-k)$ *up to homotopy. Thus, framings are in one-to-one correspondence with* $\pi_{k-1}(O(n-k))$. *We will develop a better characterization of this notion for* 4*-manifolds.*

3.2 Handle Decompositions

Let M^n be a smooth compact connected manifold, and $f : M \to \mathbb{R}$ be Morse-Smale (together with a suitable g). The proof of the following lemma can be found in [13].

Lemma 2 *The morse function* f *can be chosen so that*

- f *is self-indexing, i.e.,* $f(p_k) = k$ *for all critical points* p_k *of index* k.

- *There exists a unique index-0 critical point.*
- *If M is closed, then there exists a unique index n critical point.*

Remark 24 *The second condition can be proven via connectedness and handle cancellations, and the third one can be seen as a consequence of the second one under the dual decomposition given by $-f$.*

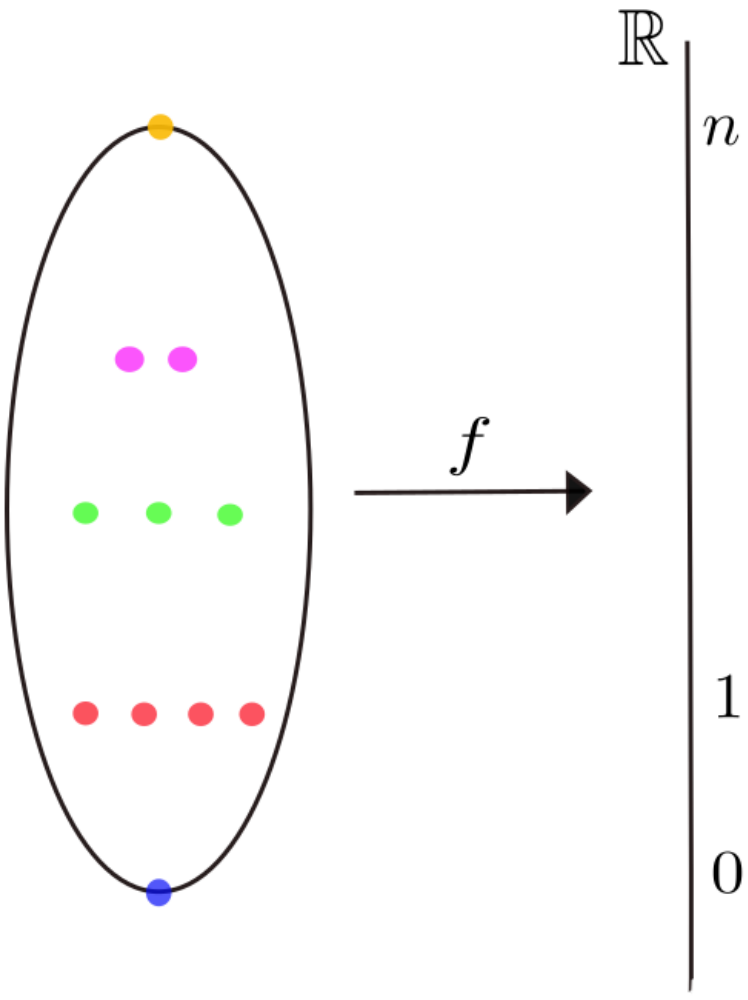

Figure 3.5: The modified morse function.

Given the above lemma, the schematic picture to have in mind is the figure 3.5. Now, we have a presentation of M in terms of handles such that handles are attached in order:

$$M = h^0 \bigcup (h_1^1 \cup \cdots \cup h_{c_1}^1) \bigcup (h_1^2 \cup \cdots \cup h_{c_2}^2) \bigcup \cdots .$$

Chapter 4

MODIFYING THE HANDLE DECOMPOSITIONS

In this chapter, we are going to talk about certain moves that change the handle decomposition but not the manifold. These moves will be creation/cancellation of geometrically complementary handles, and handle slides.

4.1 Creation/Cancellation of Geometrically Complementary Handles

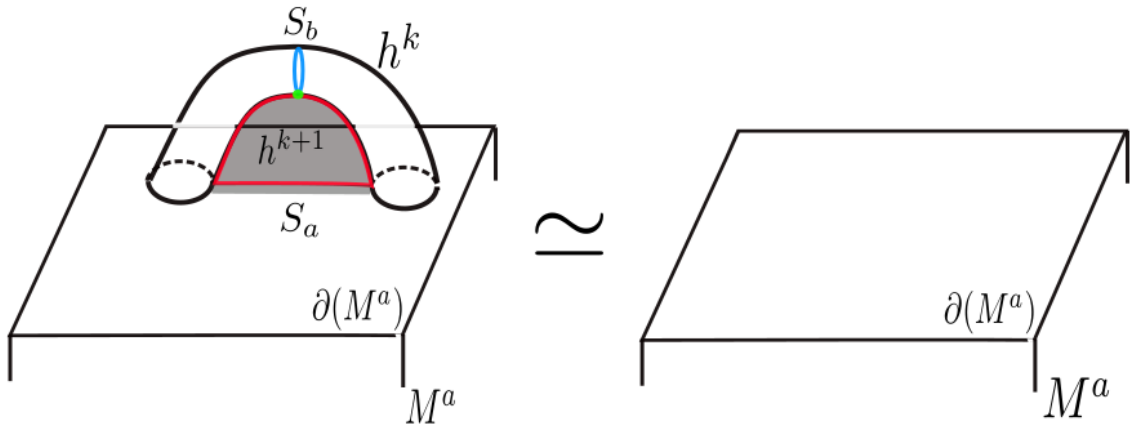

Figure 4.1: Cancellation of handles.

Given two handles h^k and h^{k+1} such that $S_b(h^k) \cap S_a(h^{k+1})$ is a singleton, then we can cancel h^k and h^{k+1} from the decomposition. Consider figure 4.1. In this figure, we see the actual handle like shape, which is the k-handle denoted by h^k, and a $k+1$-handle denoted by h^{k+1}, which is geometrically complementary to h^k,

indeed, the blue sphere and the red sphere, which denote the belt sphere of h^k and the attaching sphere of h^{k+1}, intersect at a single point, which is denoted by the green point. Then, we can see that these two handles together yield a single bump and this bump does not change the diffeomorphism type so we can delete them.

Remark 25 *There is a flow lines interpretation as well: Let p_k and p_{k+1} are the critical points corresponding to h^k and h^{k+1}, respectively. If there is a single flow line from p_{k+1} to p_k, then we can delete h^k and h^{k+1} from the handle decomposition.*

4.2 Handle Slides

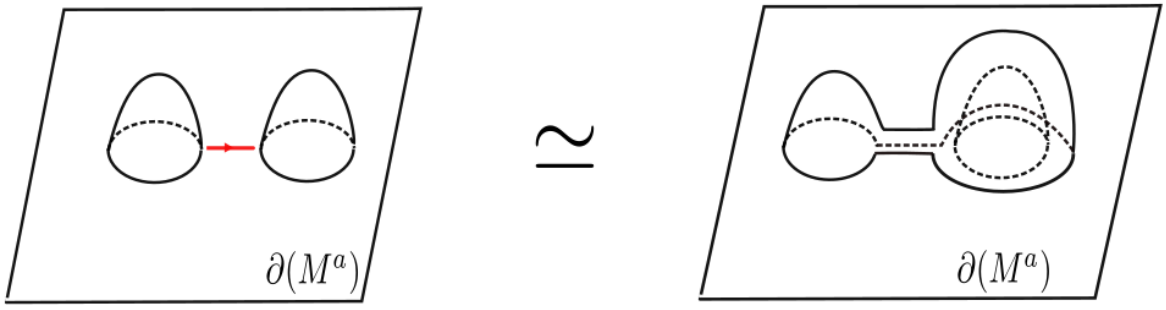

Figure 4.2: A handle slide.

Let h_1 and h_2 be handles of the same index attached to the boundary of the resulting manifold from attaching the previous handles. A handle slide of h_1 over h_2 is the operation of moving the attaching sphere of h_1 across the belt sphere of h_2 through isotopy. Isotopies do not change the diffeomorphism type, thus we can always do this. One can also think of this as follows: If one of the handles are attached, then the boundary of the resulting manifold contains the belt region of

this handle and the other handle can move freely on this portion of the boundary as well. A schematic picture is provided in figure 4.2 ; also, it is important to visualize the attaching spheres as well, a picture of this is provided in figure 4.3. We talked about these two moves, and the fact that these moves do not change

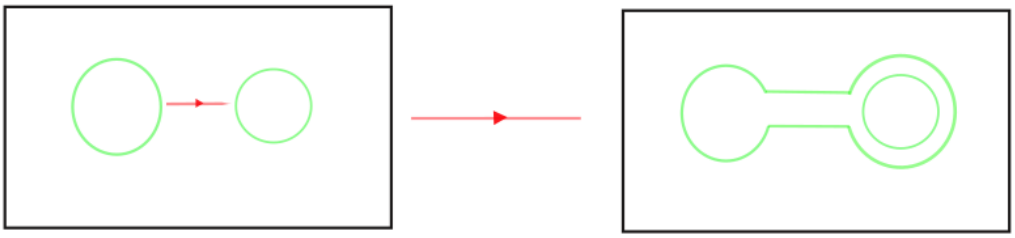

Figure 4.3: Attaching spheres under a handle slide.

the diffeomorphism type of the manifold. Interestingly, the converse is also true for compact manifolds:

Theorem 8 *Let M^n be compact. Any two handle decompositions of M can be related to each other by a sequence of*

- *creation/cancellation of geometrically complementary handles,*
- *handle slides,*
- *isotopies.*

We end this chapter by a small remark regarding dual decompositions.

Remark 26 *I mentioned about dual decomposition before but to be precise, this is the decomposition obtained by using $-f$ instead of f, which yields the original handle decomposition. The name "dual" makes sense under this change k-handles turn into $n-k$-handles, and vice versa. Moreover, cores of these k handles are co-cores of the $n-k$-handles.*

Chapter 5

HANDLE DECOMPOSITIONS IN DIMENSIONS ONE AND TWO

One can find a more detailed discussion in [11]. The handle decomposition of a smooth, connected, and closed 1-manifold contains only a single 0-handle, which is just a point, and a single 1-handle, which is a closed interval and there is a unique way to attach the 1-handle, which yields S^1.
The 2-dimensional case is visually suggestive because the schematic and the actual pictures coincide, handle slides will be actually visible. Let $M = L^2$ be a closed, connected smooth manifold. We will prove the following theorem, which gives us a classification of closed surfaces:

Theorem 9 *Any closed, connected smooth surface L is diffeomorphic to one and only one of the following:*

- $\Sigma_g, g = 0, 1, 2, \cdots$, *i.e. the closed orientable surface of genus g.*
- *The connected sum $P^2 \# P^2 \# \cdots \# P^2$ of k copies of the projective plane P^2, $k = 1, 2, \cdots$,*

The surfaces in the second item are called non-orientable closed surfaces.

By being closed and connected, there are unique 0 and 2-handles. Suppose there are k, 1-handles, i.e. $L = h^0 \bigcup (h_1^1 \cup h_2^1 \cup \cdots \cup h_k^1) \bigcup h^2$. If $k = 0$, then we are attaching the 2-handle, which is a disk, to the 0-handle, which is also a disk along their boundaries, we obtain a manifold diffeomorphic to S^2 (there are no exotic structures in dimension 2). If $k = 1$, by the Morse inequalities, we actually know that this surface cannot be Torus, since it requires at least 4-handles. In fact, one can find a morse function on the projective plane with 3-critical points (see example

3.8 of [11]). We will now see that there is a unique L with a single 1-handle, so this has to be the projective plane, and this will also show why the torus cannot be obtained by using three handles. Consider figure 5.1. This figure shows two

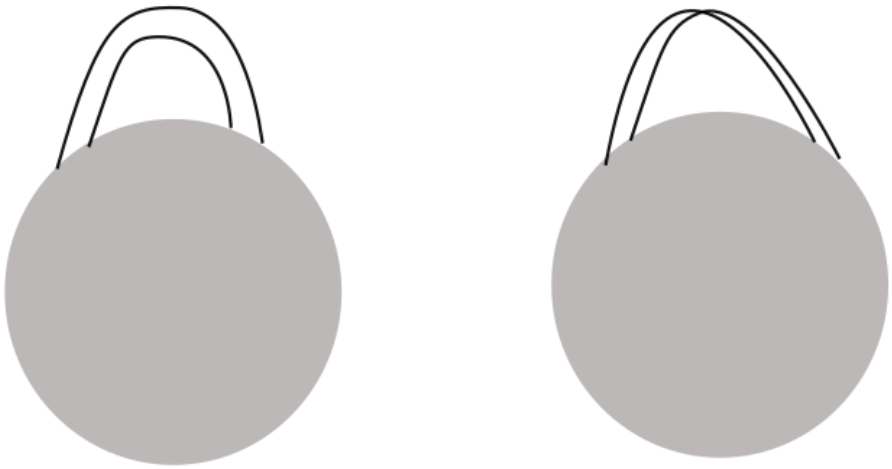

Figure 5.1: Attaching a 1-handle in dimension 2.

ways to attach a 1-handle to a 0-handle, the one on the right is half-twisted. In fact, these are the only ways since $\pi_{k-1}(O(n-k)) = \pi_0(O(1)) = \pi_0(S^0) = \mathbb{Z}_2$. This also makes sense visually since if one wants to add a further half-twist in the same direction, then one obtains the same picture with a different embedding of the annulus. Note that the manifold on the left cannot be capped of by using a single 2-handle since it has two boundary components. However, the one on the right can be capped of and this shows that there is a single closed surface whose handle decomposition contains a single 1-handle. Since P^2 has such a decomposition, this is P^2. Now, we try to understand $k = 2$. There are two cases, where both handles are attached in the orientation-preserving way (without half-twists), and the case where at least one of the handles are attached in an orientation-reversing manner. Suppose now that one of the handles is attached in an orientation-reversing manner. If the attaching region of the other handle is crossed with the orientation-reversing one, they can be uncrossed by sliding the handles. See figure 5.2. Therefore, we

may assume that the 1-handles are not crossed. Now, notice that, to obtain a closed manifold we need both of these handles to be orientation-reversing if one of them is orientation-preversing we have the same problem: we cannot cap it off. In that case, we have $P^2\#P^2$ (also known as the Klein bottle). If both are orientation-preserving (their attaching regions should be crossed to obtain a closed surface), as discussed in the preliminaries chapter, we obtain the torus. In the case $k = 3$, the boundary

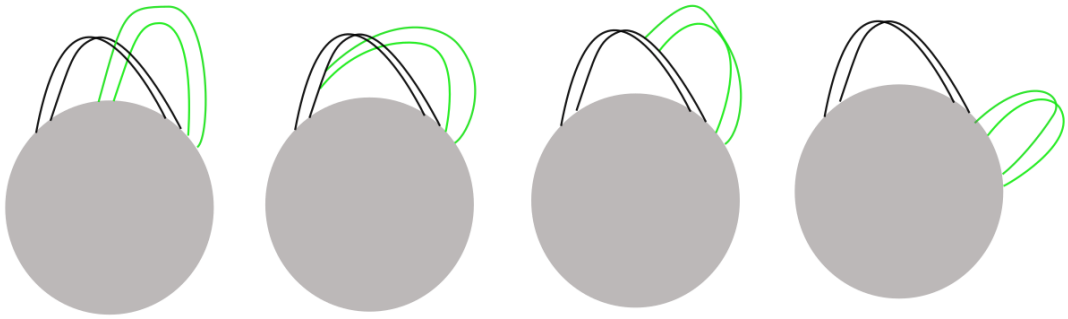

Figure 5.2: Uncrossing 1-handles.

$\partial(h^0 \cup h^1_1 \cup h^1_2 \cup h^1_3)$ is disconnected if all three handles are orientation-preserving, so at least one of them has to be orientation-reversing, in which case, we can slide off of the attaching regions of the other handles as done in the 5.2. There are two cases (that can be capped off) as depicted in figures 5.3 and 5.4. The one in figure 5.3 can be capped off to obtain $P^2\#P^2\#P^2$, and the one in figure 5.4 can be capped off to obtain $P^2\#T^2$. Note also that they are diffeomorphic since in figure 5.4, one can slide the orientation-preserving handles off of each other to obtain the first case. The general case follows from handleslides and similar arguments: If there are orientation-reversing 1-handles and if there are even number of 1-handles, then we obtain $T^2\#\cdots\#T^2$, where the number T^2's is equal to $k/2$. If there is one orientation-reversing handle, then we have $P^2\#\cdots\#P^2$, where the number of P^2's is k.

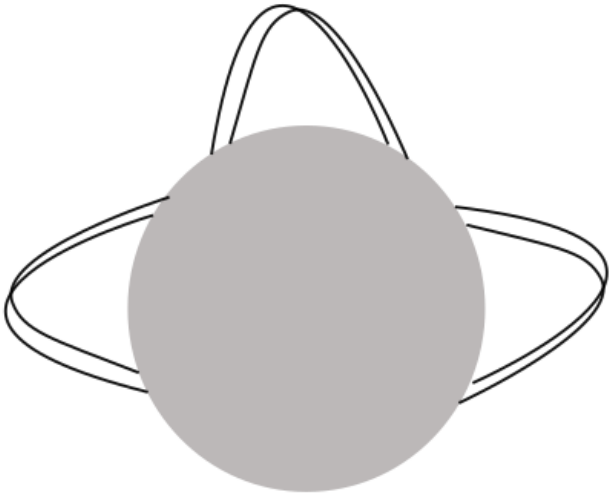

Figure 5.3: Three orientation-reversing 1-handles.

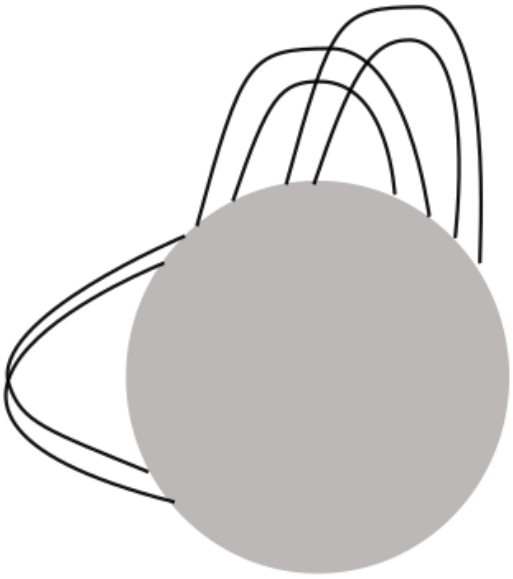

Figure 5.4: Three 1-handles, one is orientation-reversing.

Chapter 6

HANDLE DECOMPOSITIONS IN DIMENSION THREE: HEEGAARD SPLITTINGS

This will be a very brief introducing, see [11], for instance, for the details. Let $M = Y^3$ be a closed, connected, orientable smooth manifold.

Lemma 3 $\chi(Y) = 0$.

Proof $\chi(Y) = b_0(Y) - b_1(Y) + b_2(Y) - b_3(Y)$, *but by the Poincaré duality,* $b_0(Y) = b_3(Y)$ *and* $b_1(Y) = b_2(Y)$, *thus* $\chi(Y) = 0$.

By the above lemma (or the proof of it), and the fact that Y is connected and closed, it follows that the handle decomposition of Y has a single 0 and 3-handles and if it has g 1-handles, then it also has g 2-handles. Let $U_\alpha = f^{-1}((-\infty, \frac{3}{2}])$. U_α is called a genus-g handlebody, which is D^3 with g, 1-handles are attached in the unique orientable way.

Remark 27 *Since framings are in one-to-one correspondence with* $\pi_{k-1}(O(n-k))$, *it follows in our case that they are parametrized by* $\pi_0(O(2)) = \mathbb{Z}_2$. *One of such framings makes the resulting manifold orientable, we choose this one as in the case of closed surfaces. We will see that the situation in dimension* 4 *is more complicated, and in that case we actually need to deal with framings (for attachments of* 2*-handles).*

The goal is to describe $Y = U_\alpha \cup_\Sigma U_\beta$. Figure 6.1 shows a schematic diagram. Note that $\partial(U_\alpha) = \Sigma$ is an orientable surface of genus g. In general, let $\alpha = \{\alpha_1, \cdots, \alpha_g\}$ be the belt spheres of the 1-handles, denote by the blue circles in 6.1. Note that α is a set of g pairwise disjoint simple closed curves which are linearly independent in $H_1(\Sigma)$. To describe U_β, we turn the handle decomposition upside down: Let

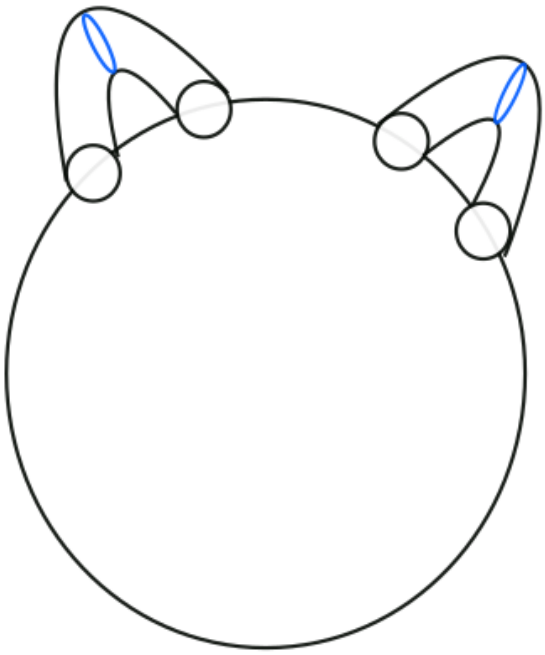

Figure 6.1: U_α consisting of two 1-handles.

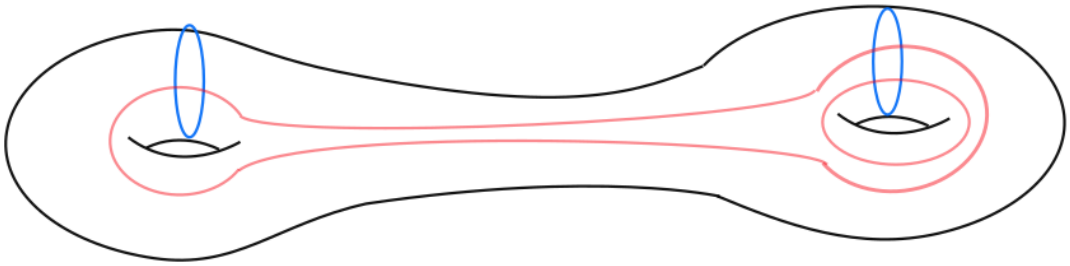

Figure 6.2: U_α and attaching spheres of U_β.

$\beta = \{\beta_1, \cdots, \beta_g\}$ be the set of belt spheres of the dual 1-handles, which are the attaching spheres of the original 1-handles. Note that on $\Sigma = \partial(U_\alpha)$, β might be quite complicated, see figure 6.2 for an example.

Definition 18 *A Heegaard diagram is a triple* (Σ, α, β) *such that* Σ *is closed ori-*

ented surface of genus g, and α and β are sets of g pairwise disjoint linearly independent simple close curves on Σ.

Theorem 10 *A Heegaard diagram (Σ, α, β) defines a closed, oriented, connected 3-manifold Y up to diffeomorphism. Moreover, every closed, oriented, connected 3-manifold Y can be represented with a Heegaard diagram.*

Example 10 *The Heegaard diagrams in figure 6.3. The one on the right corresponds to gluing of two solid tori $S^1 \times D^2$ along their D^2's, which yields $S^1 \times S^2$. The one on the left is S^3.*

Figure 6.3: Two Heegaard diagrams.

Remark 28 *$Y = U_\alpha \cup_\Sigma U_\beta$, is called a Heegaard splitting of Y. Moves that relates different diagrams such as creation/cancellation of geometrically complementary handles have particular names in this context such as (de)stabilizations, α-handle slides.*

Chapter 7

HANDLE DECOMPOSITIONS IN DIMENSION FOUR

Let $M = X^4$ be orientable and connected. given a self-indexing morse function f on X, set $X|_k = f^{-1}(-\infty, k+\frac{1}{2})$. Since X is connected there is a unique 0-handle $D^0 \times D^4 \simeq D^4$. The 1-handles will be attached to the boundary of this 0-handle, which is S^3, which is the one-point compactification of $\mathbb{R}^3$. There are again two ways to attach the 1-handles, we choose the orientable one. The attaching region of a 1-handle is $S^0 \times D^3$, which is just two balls. Therefore, we are actually attaching two D^3's. Figure 7.1 shows these two 3-balls, the dotted line shows that these two 3-balls are related and this is important if we have more than one 1-handle. If we

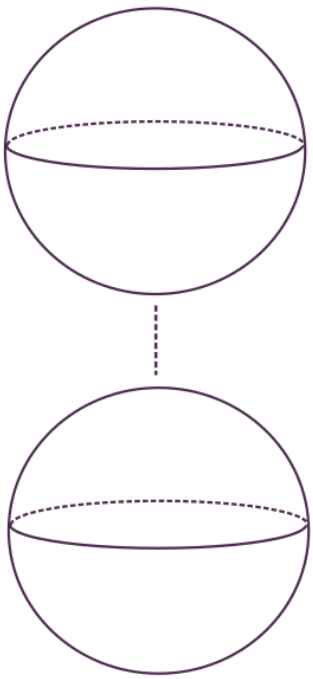

Figure 7.1: The attaching spheres of a 1-handle.

attach a single 1-handle, then $X|_1$ is a union of D^4 and $D^1 \times D^4$, and if we view

$D^4 \simeq D^1 \times D^3$, we have the picture shown in figure 7.2. It is clear from the figure that the resulting manifold with boundary is $S^1 \times D^3$. Furhermore, if we have c_1

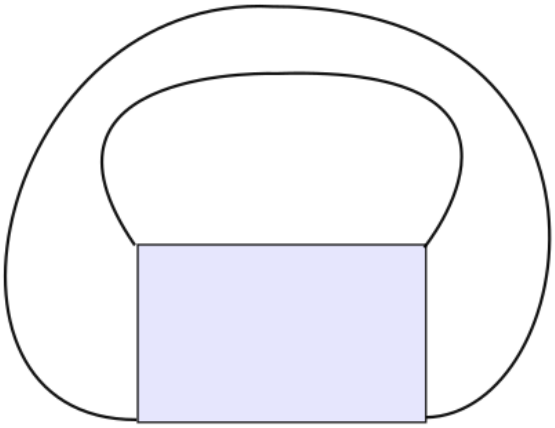

Figure 7.2: A 1-handle attached to a 0-handle.

1-handles in total, then $X|_1 \simeq \natural^{c_1}(S^1 \times D^3)$, where $\natural$ denotes the boundary connected sum. Also, $\partial(X|_1) = \#^{c_1}(S^1 \times S^2)$. Now, the attaching spheres of 2-handles are $S^1 \subset \#^{c_1}(S^1 \times S^2)$. To understand 2-handle attachments, we need to talk about links and knots.

Definition 19 *A knot K in Y, where Y is a 3-manifold without boundary, is a closed, connected 1-submanifold of Y considered up to isotopy. If we drop the connectedness condition, we obtain a link instead of a knot.*

Example 11 *In figure 7.3, we see the Trefoil knot on the left and the Hopf link on the right.*

We now attach the 2-handles along a link $L \subset \#^{c_1}(S^1 \times S^2)$. For instance figure 7.4 shows the attaching sphere of a two handle, where there are two 1-handles present. The dotted line notation becomes important. In this figure, the red arrows do not show the orientation of the link but it actually shows how it is located, at least its picture in the attaching region. We see that if it enters at a point in one of the

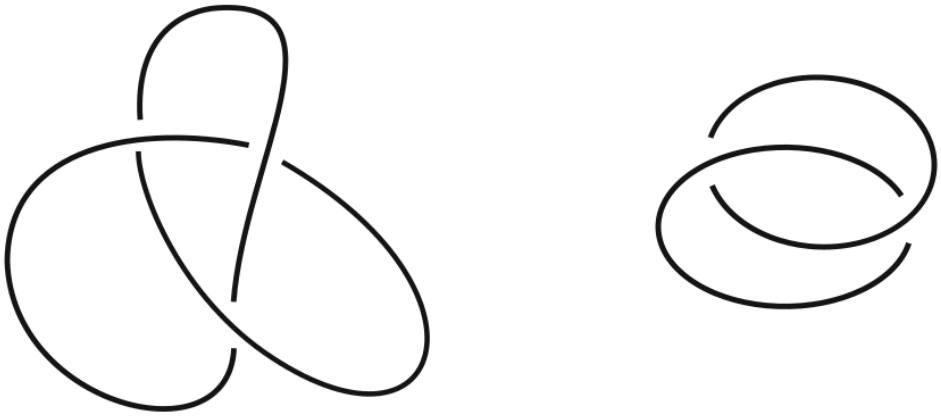

Figure 7.3: The trefoil knot and the Hopf link.

balls D^3, it pops up in the ball forming the 1-handle with the original ball, at the reflection point. There is one more representation of the figure 7.4, which is easy to draw but describes exactly the same thing, that is called the dotted circle notation. See [2] for learning more about this notation. In figure 7.5, we see this notation. Of course, there is no need to draw it this large now, it is just for comparing with 7.4. However, note that since $\pi_1(O(2)) \simeq \mathbb{Z}$, the framings are important now and we need a way to deal with them. So, the link itself is no longer sufficient. Recall that a framing is a diffeomorphism $\nu(S^1_a) \to S^1_a \times D^2$ up to isotopy. It is determined by a longitude $\lambda \to S^1_a \times \{1\}$. Given $K \subset S^3$, there exists a unique longitude λ_0 null-homologous in $S^3 - K$. This longitude is called the Seifert longitude. We will talk more about this later on but for now, our goal is to understand how this is used in practice. In figure 7.6 we see a longitude of the knot in figure 7.5. We define the framing of a knot with respect to the Seifert longitude, in this case the original knot (the blackboard framing to be precise) has framing 0 (since it is the unknot). Also if the framing is given by the green curve, then it is -2 according to the rule given in figure 7.7. We will express this in a better form in the following chapters. The following theorem is quite important because it allows us not to deal with 3 and

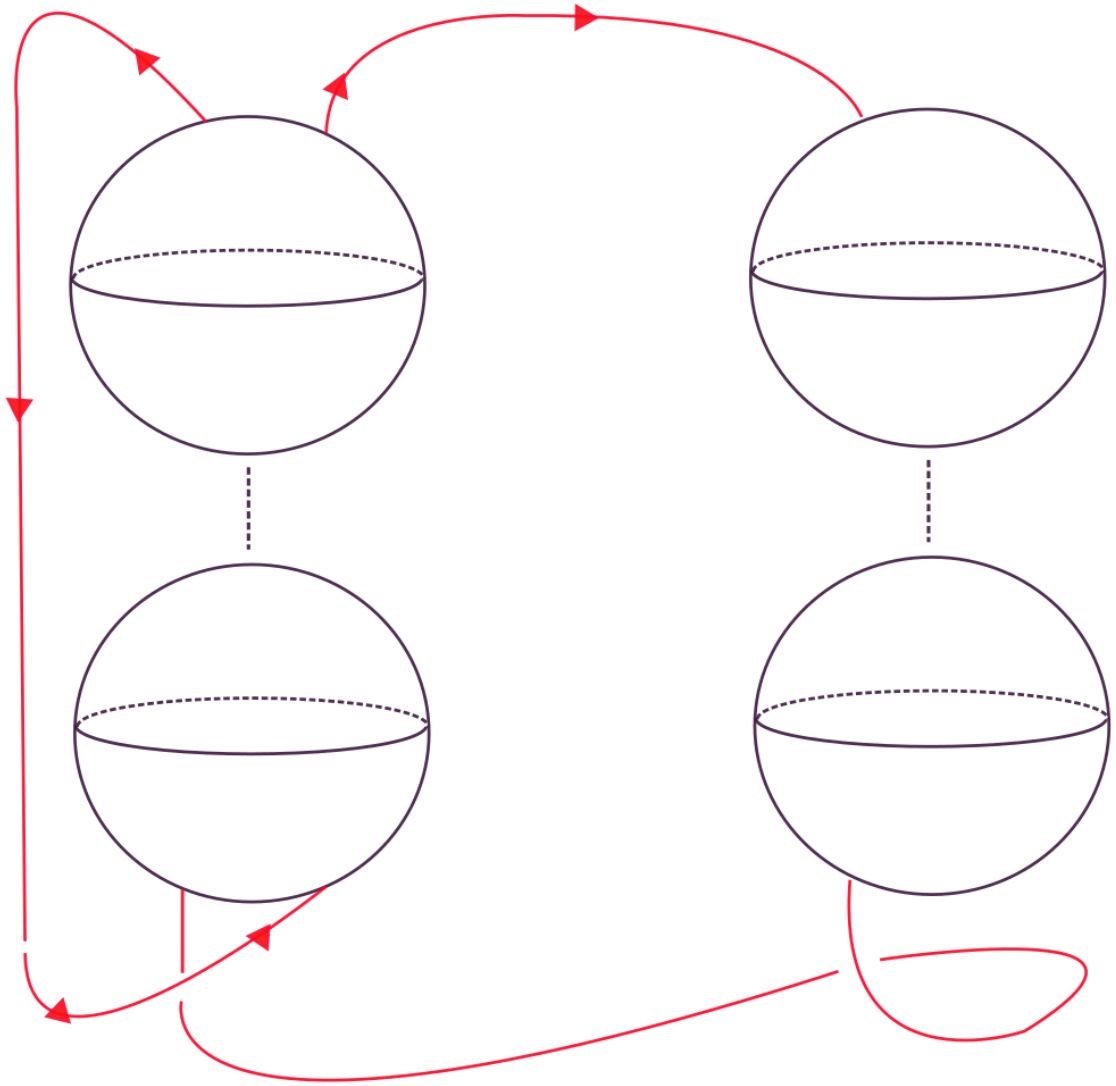

Figure 7.4: The attaching sphere of a 2-handle.

4-handles. This is a theorem of Laundenbach and Poenaru [9].

Theorem 11 *Every diffeomorphism of* $\#^r(S^1 \times S^2)$ *extends to* $\natural^r(S^1 \times D^3)$.

As a result of this theorem, there is a unique way to attach the 3-handles and 4-handles. Using this, we can consider figure 7.5 as a closed 4-manifold.

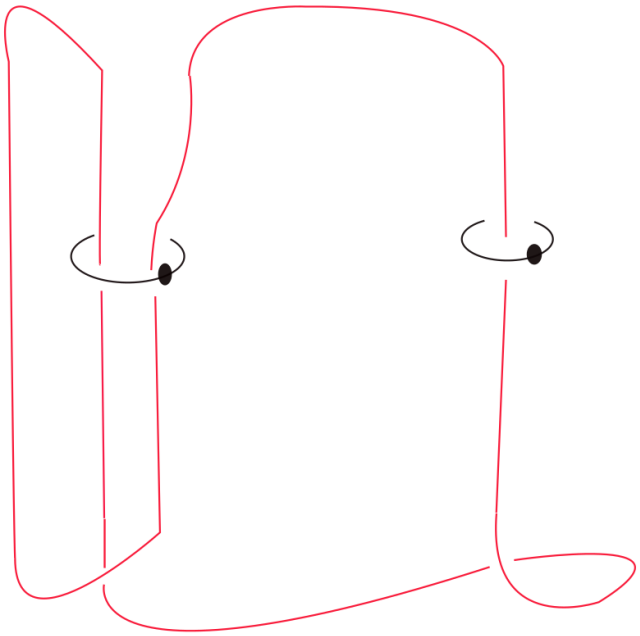

Figure 7.5: The attaching sphere of a 2-handle with the dotted circle notation.

Remark 29 *In fact, figure 7.5 can describe three objects:*

- *The* 4*-manifold* $X|_2$*,*
- *The closed* 4*-manifold obtained by using the theorem above,*
- *The* 3*-manifold* $\partial(X|_2)$*. This diagram is named as the Kirby diagram.*

Note that a theorem of Lickorish and Wallace says that actually every 3-manifold can be represented as $\partial(X|_2)$.

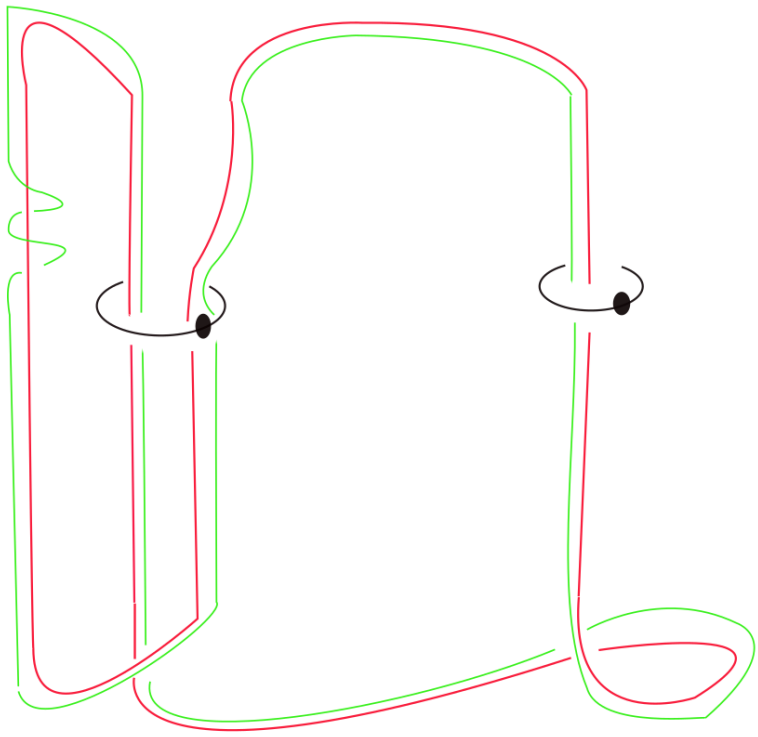

Figure 7.6: A longitude (framing) of a knot.

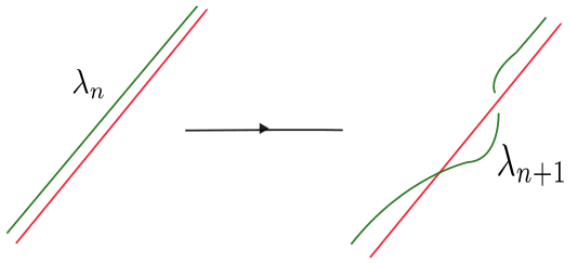

Figure 7.7: The framing rule.

Chapter 8

RELATING DIFFERENT DIAGRAMS: KIRBY CALCULUS

We already know that any two handle decompositions of X are related by a sequence of handle slides, creation/cancellation of geometrically complementary handles. Now, we can actually see how these look like in dimension 4. Figure 8.1 depicts the handle slides move. Here the picture on top depicts a handle slide between two 1-handles and the second figure shows a handle slide of 2-handles. In this figure, if the knots have framings a and b as shown. Then, while doing the handle slide, the framing of the second one does not change, but the first one has b additional twists along the second one (in the figure there is only one), and it also goes around b so the framing of the first handle is now $a + b \pm 2 \times lk(k_1, k_2)$, where $lk(k_1, k_2)$ is the linking number between the given knots, which we will talk about in the next chapter. Handle creations/cancellations are easier to see in Kirby diagrams,

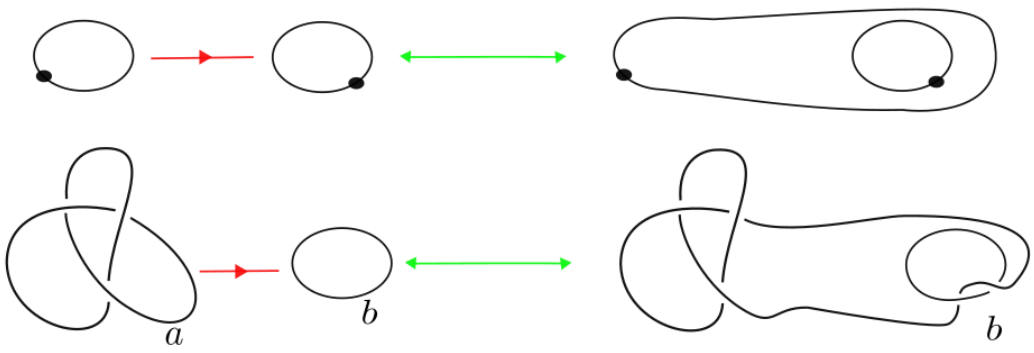

Figure 8.1: Handle slides in Kirby diagrams.

a 1-handle and a 2-handle cancel out if the two handle goes through the 1-handle

once and if there are no other two handles going through the 1-handle. In the figure 8.2, we see two such geometrically complementary handles cancel out. Note also that these two moves together are necessary and sufficient. As noted before, we can

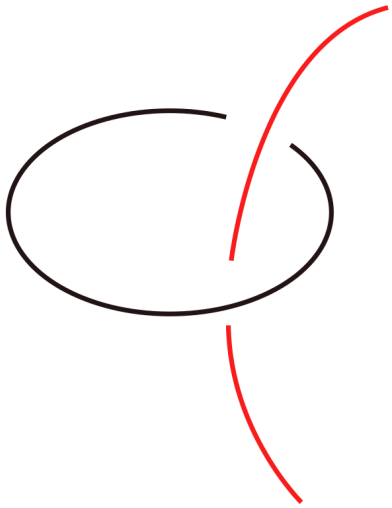

Figure 8.2: Cancellation of geometrically complementary handles.

consider the 3-manifold $\partial(X|_2)$. We need to talk about two more moves to give a precise statement. One can always create (or remove) an unknot with framing ± 1, this does preserve the diffeomorphism-type of $\partial(X|_2)$. However, note that this move changes the 4-manifold. Creation of such a handle is called *blow up* and removing it is called *blow down*. See figure 8.3. The next move is called the zero-dot surgery and it will be important for us to understand the main result. As the name suggests, it allows us to interchange the dot and the 0 for a given unknot. See figure 8.4. Now, we can state the following theorem.

Theorem 12 *Any two descriptions of Y^3 as $\partial(X|_2)$ are related by handleslides, creations/cancellations of geometrically complementary handles, blow-ups (downs), and zero-dot surgeries.*

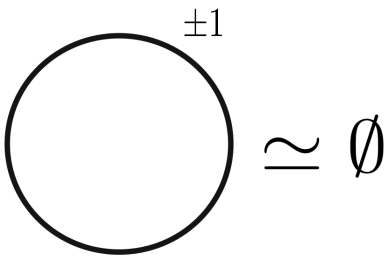

Figure 8.3: Blow up and down operations.

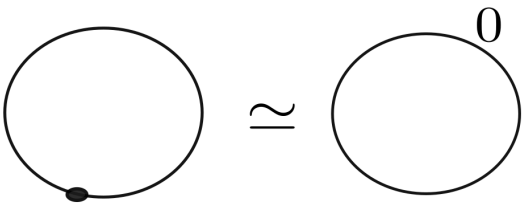

Figure 8.4: Zero-dot surgery.

Chapter 9

FURTHER NOTES

In this chapter, I will be explaining how to read off some algebraic invariants from the diagram, and also I will talk a bit about the framing and the linking number as mentioned in the previous chapters.

9.1 Handles, Homotopy, and Homology

The main idea to read off the algebraic topology of X is to observe that, up to homotopy, a handle decomposition collapses onto a cell decomposition. Roughly, each k-handle $D^k \times D^{n-k}$ collapses onto the k-cell $D^k \times 0$, dragging all later cell attachments along by homotopy.

Example 12 *Suppose that X consists only of one 0-handle and m handles of index $k = 1$ (or 2), then by collapsing the 0-handle to a point, X is homotopy equivalent to an m-fold wedge of k-dimensional spheres, i.e. $\bigvee^m S^k$.*

Let X be any smooth, connected, 4-manifold with a handle decomposition that has a unique 0-handle. Moreover, assume that handles are attached in order of increasing index and that all handles of a given index are attached simultaneously. Note that $\pi_1(X)$ is determined by $X|_2$:

- generators are the 1-handles, each represented by an oriented core curve for a 1-handle.

- relations are given by 2-handles: we express the oriented attaching curves as words in the 1-handles' core curves.

This turns out to be independent of the framings of the 2-handles. Moreover, by abelianizing, one can compute $H_1(X)$ as well. Let's go over these via the following example.

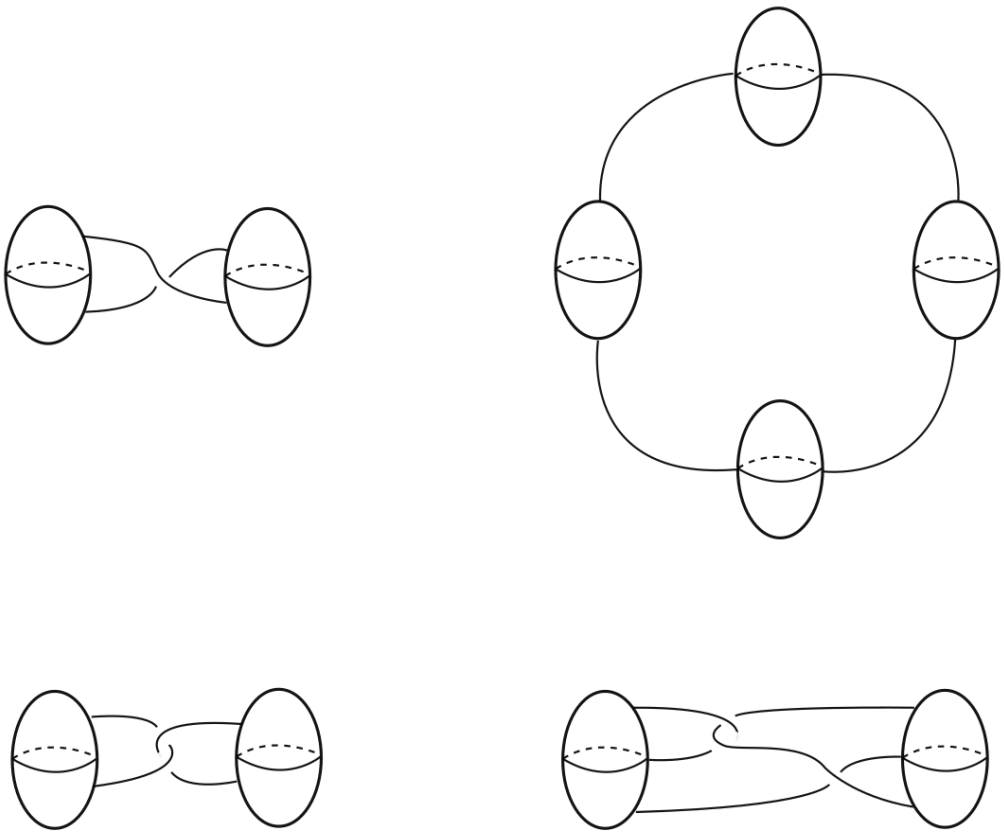

Figure 9.1: Some Kirby diagrams.

Example 13 *Consider the handle diagrams in figure 9.1. In the clockwise order starting from the upper-left corner:* $\pi_1(X) \simeq \langle x|x^2\rangle \simeq \mathbb{Z}/2\mathbb{Z}$, $\pi_1(X) \simeq \langle x, y|xyx^{-1}y^{-1}\rangle \simeq \mathbb{Z} \oplus \mathbb{Z}$,$\pi_1(X) \simeq \langle x|xx^{-1}x\rangle \simeq 1$, $\pi_1(X) \simeq \langle x|xx^{-1}x\rangle \simeq 1$ $\pi_1(X) \simeq \langle x|xx^{-1}\rangle \simeq \mathbb{Z}$.

Note also that, directly from this description of the fundamental group, one can show that

- There exist 4-manifolds that has a nonabelian fundamental group.
- Every finitely presented group arises as the fundamental group of a smooth, compact, orientable 4-manifold.
- The previous item is also true for closed 4-manifolds. (One can double the manifold in the previous item together with some observations).

One can compute the homology groups $H_k(X)$ by using cellular homology: $C_k(X)$ is generated by k-handles, and the boundary formula for a k-handle h is given by

$$\partial h = \sum (B_i \cdot A) h_i,$$

where A is the attaching sphere of the k-handle h, B_i is the belt sphere of the $k-1$-handle h_i, and $B_i \cdot A$ is their signed intersection.

Example 14 *In figure 9.1, the second homology groups in the clockwise order are:* $1, \mathbb{Z}, 1, \mathbb{Z}$.

9.2 The Linking Number

Let K_1 and K_2 be disjoint, oriented knots in S^3. Any knot complement in S^3 has $H_1 \simeq \mathbb{Z}$ and is generated by the meridian of K_1. We can define the linking number as follows:

Definition 20 *The linking number of* K_1 *and* K_2*, denoted by* $lk(K_1, K_2)$*, is equal to* $[K_2] \in H_1(S^3 \setminus K_1) \simeq \mathbb{Z}$.

Remark 30 *The linking number can be computed in different ways:*

- *From the diagram,* $lk(K_1, K_2) = \frac{1}{2} \sum \{$*signed crossings between* $K_1, K_2\}$*, where the signs are determined via the right-hand rule as in figure 9.2. This also shows that the linking number is symmetric, i.e.* $lk(K_1, K_2) = lk(K_2, K_1)$.

- *The class* $[K_2] \in H_1(S^3 \setminus K_1) \simeq \mathbb{Z}$ *can be calculated by choosing an oriented Seifert surface (see the last chapter)* Σ_1 *for the oriented knot* K_1*, perturbing* K_2 *to be transverse to* Σ_1*, then counting the signed intersection number* $K_2 \cdot \Sigma_1$.

Let us consider now a 4-manifold X obtained from B^4 by attaching 2-handles along a framed, oriented n-component link L. Then X is homotopy equivalent to $\bigvee^n S^2$, implying $H_2(X) \simeq \mathbb{Z}^n$. We are interested in finding a basis for $H_2(X)$. There is a natural choice. For each component K_i in L, fix a Seifert surface $\sigma_i \subset S^3$. Also, we make sure that σ_i is in general position with respect to $L \setminus K_i$. Let Σ_i be the union of

Figure 9.2: The right-hand rule.

σ_i with the core disk $D_i = D^2 \times 0$ inside the 2-handle along K_i. Then, the homology classes $[\Sigma_i]$ form a basis for $H_2(X)$. (Indeed, X collapsing to $\bigvee^n S^2$ carries Σ_i to the i^{th} wedge summand S^2.) Now, we try to understand the intersections of these closed surfaces. If $i \neq j$, then Σ_i and Σ_j intersect in S^3. Let Σ_j' be a surface obtained from Σ_j by pushing the interior of σ_j slightly into B^4 so that $\Sigma_j \cap \partial B^4 = K_j$. See figure 9.3 for a schematic picture. This new surface represents the same homology class

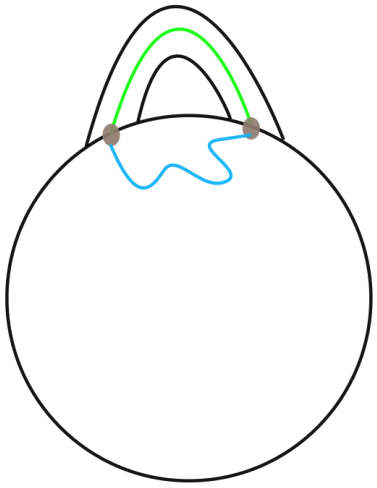

Figure 9.3: Σ_i': brown: K_i, green: D_i, blue: Push off of $int(\sigma)$.

and is transverse to Σ_i, intersecting it only where K_j intersects Σ_i. Thus, we have

$$[\Sigma_i] \cdot [\Sigma_j] = [\Sigma_i] \cdot [\Sigma_j'] = \Sigma_i \cdot \Sigma_j' = \Sigma_i \cdot K_j = lk(K_i, K_j).$$

In order to compute $[\Sigma_i] \cdot [\Sigma_i]$, we need to perturb one copy of Σ_i. In the 2-handle $D^2 \times D^2$ attached along K_i, choose a perturbed copy of the core disk, expressed as $D_i' = D^2 \times \{\epsilon\}$ for a point $\epsilon \in D^2 \setminus \{0\}$. The intersection $D_i' \cap S^3 = K_i'$ is a framed push off of K_i with framing equal to the framing of the 2-handle. Let Σ_i' denote a copy of Σ_i dragged along during the isotopy from K_i to K_i', with its interior pushed into B^4 as well. Then, as above, the intersection number is $lk(K_i, K_i')$, which is also equal to the framing of K_i. By a similar argument one can prove the following proposition.

Proposition 1 *Let X be any smooth, compact 4-manifold. Each class in $H_2(X)$ can be represented by a smoothly embedded surface in X.*

Chapter 10

STEIN-ADJUNCTION INEQUALITY

For this chapter, a more detailed discussion can be found in [15]. This book also contains a discussion of the main result that we will talk about in the following chapter of this thesis. In this chapter, I will be introducing the last ingredient towards the main result.

Definition 21 *Given a (smooth) knot $K \subset S^3$, define $g_4(K) = min\{g(\Sigma) : (\Sigma, \partial\Sigma) \hookrightarrow (B^4, S^3)$ with $\partial\Sigma = K\}$. Here, $g(\Sigma)$ denotes the genus of Σ and $g_4(K)$ is called the slice genus.*

Remark 31 *K is slice. $\iff$ $g_4(K) = 0$. $\iff$ K bounds an embedded D^2 in B^4.*

Definition 22 *K in a contact 3-manifold (Y, ξ) is Legendrian if it is tangent to ξ.*

Example 15 *Let $(Y, \xi) = (\mathbb{R}^3, ker(dz + xdy))$. Consider the front projection, $(x, y, z) \mapsto (y, z)$. If $dz + xdy = 0$, then $x = -\frac{dz}{dy}$, therefore, a negative slope means that it is closer to the positive side of the x-axis. Therefore, the negative slope indicates an overstrand. A legendrian embedding of the trefoil knot can be seen in figure 10.1.*

With this picture in mind, note that the points that look like singularities are not singularities. They are points of vertical tangencies of the knot. Also, since overstands have more negative slope, given any knot diagram, one can keep such strands and by making the move described in 10.2, one can obtain a Legendrian embedding of the knot.

10.1 Slice-Bennequin Inequality

Now, I will only the state the versions of the statements that we will be using. I will also state a result from [7]. The following inequality is known as the Slice-Bennequin

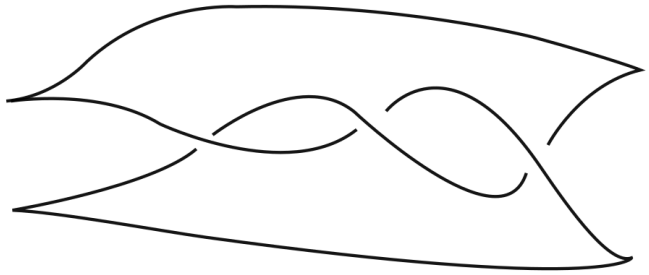

Figure 10.1: Projection of the trefoil as a Legendrian embedding.

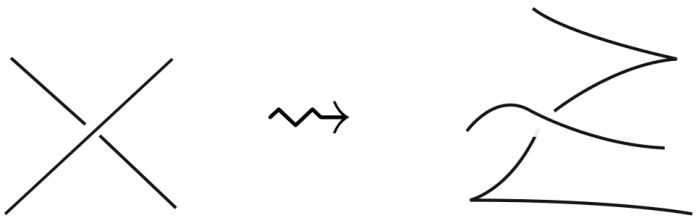

Figure 10.2: Move for turning a knot diagram into a Legendrian embedding.

inequality.

Theorem 13 *Given an oriented Legendrian representation of a knot K, let $w(K)$ denote the writhe of K and c, d, u denote the number of cusps, down cusps and up cusps, respectively. Then the following inequality holds:*

$$2g_4(K) - 1 \geq w(K) - \frac{c}{2} + \frac{1}{2}|d - u|.$$

Example 16 *For the trefoil knot, see figure 10.1, $u = d = 2$, $w(K) = 3$, and $c = 4$. Thus, $2g_4(K) - 1 \geq 1 \implies g_4(K) \geq 1$. Note that in fact $g_4(K) = 1$, since the punctured torus with one boundary component is a Seifert surface for the trefoil knot.*

A *Stein surface* Z is a complex surface admitting a holomorphic embedding to $\mathbb{C}^N$ for some N. Compact version is called a Stein domain X which is given by $X = Z \cap B_r^{2N}$

for some B_r^{2N}. The following inequality is known as the adjunction inequality:

Theorem 14 *If $[\Sigma] \neq 0 \in H_2(X)$, where X^4 is a Stein domain and $\Sigma \hookrightarrow X$ is smooth, then*

$$[\Sigma] \cdot [\Sigma] + |\langle c_1(X), [\Sigma] \rangle| \leq 2g(\Sigma) - 2,$$

where $c_1(X)$ denotes the first Chern class of X.

There is a handle theory for Stein domains/surfaces as well. The following result will make sure that we will be able to use the above inequality.

Theorem 15 *Let X be a 4-manifold obtained by attaching 2-handles along a framed link L to B^4. If for each component K of the link L, the framing is equal to $w(K) - \frac{c}{2} - 1$, then X is Stein.*

Remark 32

- *The above result is due to Eliashberg, it also appears in [7].*
- *As we noted before, $[\Sigma_i] \cdot [\Sigma_i]$ is equal to the framing of K_i.*
- *$\langle c_1(X), [\Sigma] \rangle = \frac{1}{2}|d - u|$ (or a combination for each component given by the homology representation of the surface in terms of the handles).*

Chapter 11

THE MAIN RESULT

In this chapter, we are going to state and prove the main result. I will skip some of the diagram related/computational discussions to the last chapter in order to keep the focus on the core of the proof.

Definition 23 *A knot trace $X_n(K)$ is a 4-manifold constructed by attaching a 2-handle along K with framing n to B^4.*

The following theorem is the main result.

Theorem 16 *There exist knots K, J such that $X_n(K)$ is homeomorphic to $X_n(J)$ but not diffeomorphic to it.*

Remark 33 *In fact, it is true that there exists such knots for any given $n \geq 0$.*

Let's first give an outline of the proof: There will be two steps, we will first show that $X_n(K)$ is homeomorphic to $X_n(J)$. The second step is to show that they are not diffeomorphic. For the first step we will construct K and J as shown in figure 11.1, where Z and Z' are contractible. We are going to glue these to W via f and f'. The reason why we want to insist on the fact that Z and Z' are contractible is the following theorem of Freedman [18]. This theorem tells us that homeomorphisms between the boundaries of contractible manifolds extend to homeomorphisms between the manifolds themselves.

Theorem 17 *For two compact and contractible 4-manifolds Z and Z' with $\delta : \partial Z \to \partial Z'$ a homeomorphism. There exists a homeomorphism $\Delta : Z \to Z'$ such that $\Delta|_\partial = \delta$.*

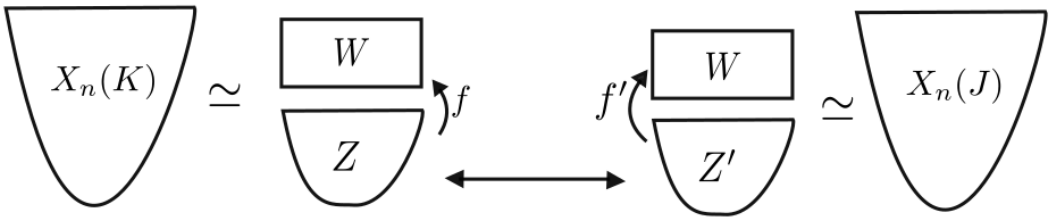

Figure 11.1: A schematic picture of the idea.

In our case, $(f')^{-1} \circ f : \partial Z \to \partial Z'$ is a homeomorphism and therefore, by the theorem above, we have a homeomorphism $F : Z \to Z'$. We define the following function:

$$\phi(x) = \begin{cases} x & \text{if } x \in W \\ F(x) & \text{if } x \in Z \end{cases}$$

We need to check that $f^{-1}(p)$ is mapped to $(f')^{-1}(p)$, i.e. $\phi(f^{-1}(p)) = (f')^{-1}(p)$. This is true since $F = (f')^{-1} \circ f$ on ∂Z. Thus F is a homeomorphism. For step 2, we are going to show that there is a smoothly embedded genus g surface in $X_n(K)$ generating $H_2(X)$ and by using the adjunction inequality we will show that there can be no such surface in $X_n(J)$.

Before starting doing all of the above, let's take a look at the following corollary as well:

Corollary 1 *There exist contractible 4-manifolds Z and Z' with a homeomorphism $\Delta : Z \to Z'$ but there does not exist a diffeomorphism $\phi : Z \to Z'$ such that $\phi|_\partial = \Delta|_\partial$.*

Proof *If there were such a ϕ, then F would be a diffeomorphism.*

Remark 34

- *A result as above is called a relative exotica result.*

- *Note that actually Z and Z' are diffeomorphic.*
- *Let $\psi : Z \to Z'$ be a diffeomorphism, then $\psi|_\partial \circ (f')^{-1} \circ f : \partial Z \to \partial Z$ does not extend to a diffeomorphism. So, in fact, Z is relatively exotic with itself.*

Now, I will introduce Z. The contractible manifold Z is given in figure 11.2. By

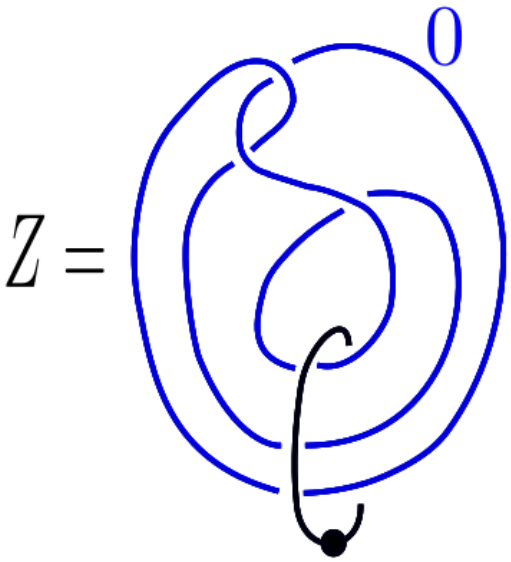

Figure 11.2: Z.

techniques introduced in the previous chapters, $\pi_1(Z) = 1$ and $H_*(Z) = H_*(B^4)$. Therefore, Z is contractible (see the next chapter for computations). Now, recall that the zero-dot surgery preserves the boundary, so we immediately have our Z' as well. So, if we apply this zero-dot surgery and using isotopy, we can say that Z' is as in the figure 11.3. Therefore, now we have two contractible manifolds Z and Z' with a homeomorphism between their boundaries given by the zero-dot surgery. Also, note that since Z and Z' have the same diagram, they are actually diffeomorphic as stated before. Now, let us define X and X'. X and X' are given as in figures 11.4, and 11.5, respectively. Now, note that, according to the argument put forward

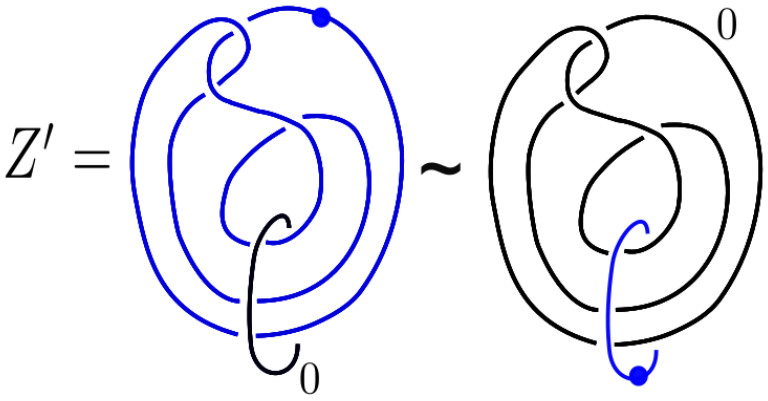

Figure 11.3: Z'.

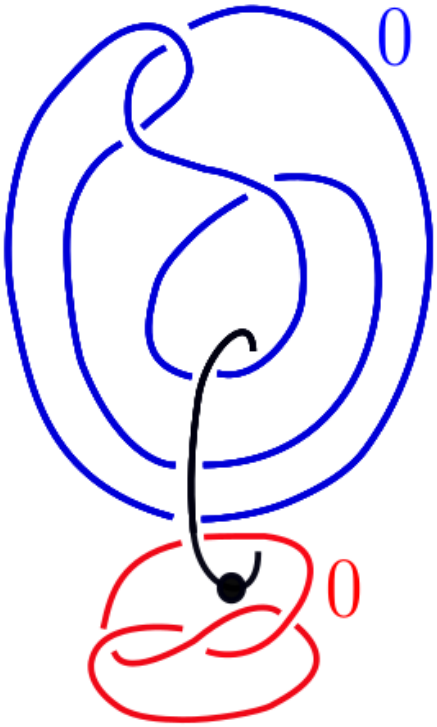

Figure 11.4: X.

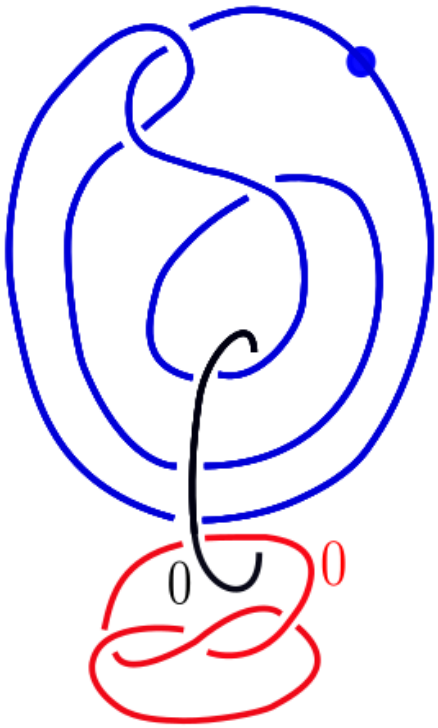

Figure 11.5: X'.

before, we know that X and X' are indeed homeomorphic. Moreover, they are both homotopy equivalent to S^2 since they are both obtained by attaching a 2-handle to a contractible manifold. To complete the proof, there are three statements, remaining to show:

- X, X' are knot traces.
- There exists $T^2 \hookrightarrow X'$ generating $H_2(X')$.
- There does not exist $T^2 \hookrightarrow X$ generating $H_2(X)$.

To prove the second item, note that X' can be seen as in figure 11.6. Again, by a previous discussion, H_2 is generated by the red 2-handle, since, this 2-handle is not linked to the 1-handle. Therefore, the Seifert surface for the trefoil whose interior is pushed into B^4 is the desired T^2 (see the next chapter for the details). We talked

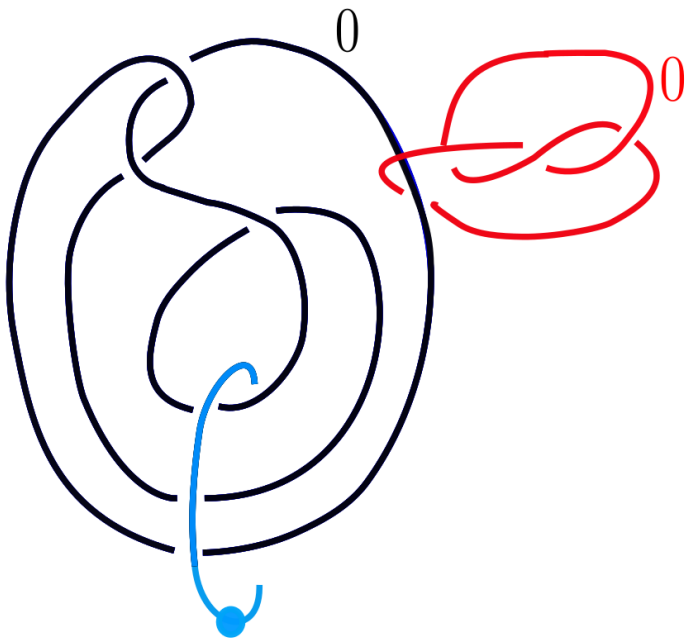

Figure 11.6: Another description of X'.

about this before in a more general manner but in figure 11.7, we see the schematic picture for this particular setting. In this picture, the union of the orange portion and the green portion is the desired surface. In this figure, I denoted the 1-handle using the "carved out" notation. This also provides insights into why there cannot be such a surface along the blue 2-handle, since the surface cannot be pushed off inside B^4 as that portion of the space is carved out. Nevertheless, this proof is also somewhat schematic. In the last chapter, I will actually construct the surfaces explicitly. I will also prove the first item in that section, which consists of many handle slides, but the idea is very straightforward, we will cancel the 1-handle with one of the 2-handles after making sure that they are geometrically complementary. So, we will end up with a diagram consisting of a single 2-handle, which is precisely the definition of a knot trace. Now, let's prove the third and the last item. So, the goal is to prove that there is no smoothly embedded surface in X generating $H_2(X)$. To do that, we are going to use the adjunction inequality, and in order to use that

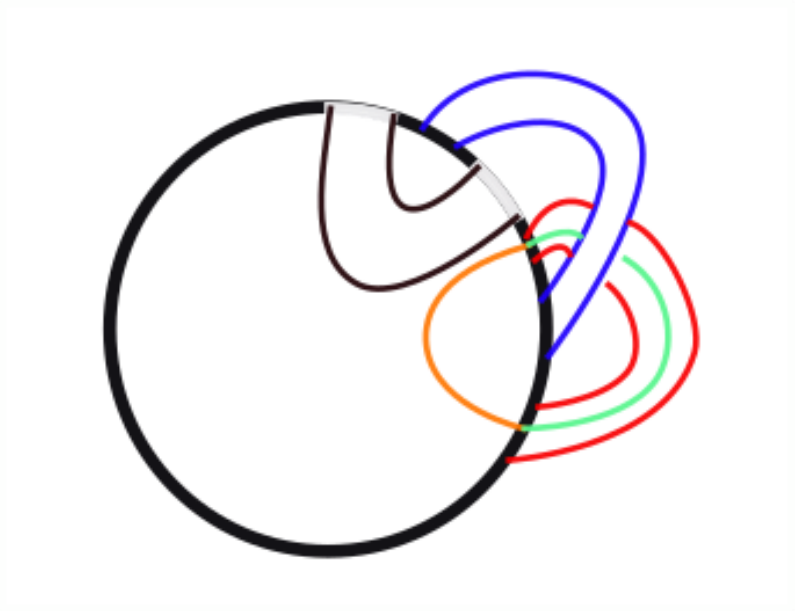

Figure 11.7: X' has a T^2 generating H_2.

inequality we need to make sure that the framing related condition is satisfied. Note that X can be described as in figure 11.8. According to the description in figure

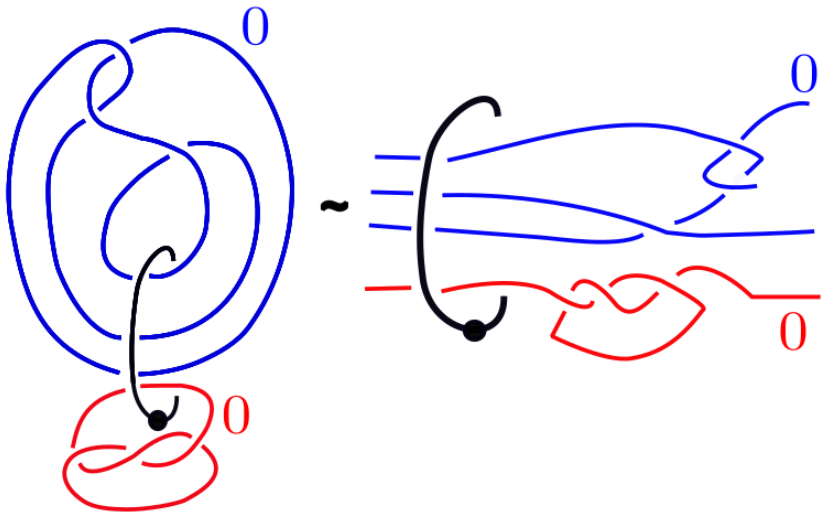

Figure 11.8: Another description of X.

11.8, framing $= w(K) - \frac{c}{2} - 1$ is not true. We cannot use the adjunction inequality. However, this is an easy issue to resolve, we can add additional cusps to reduce the right-hand side. Indeed, in figure 11.9, now this equality is satisfied. The adjunction

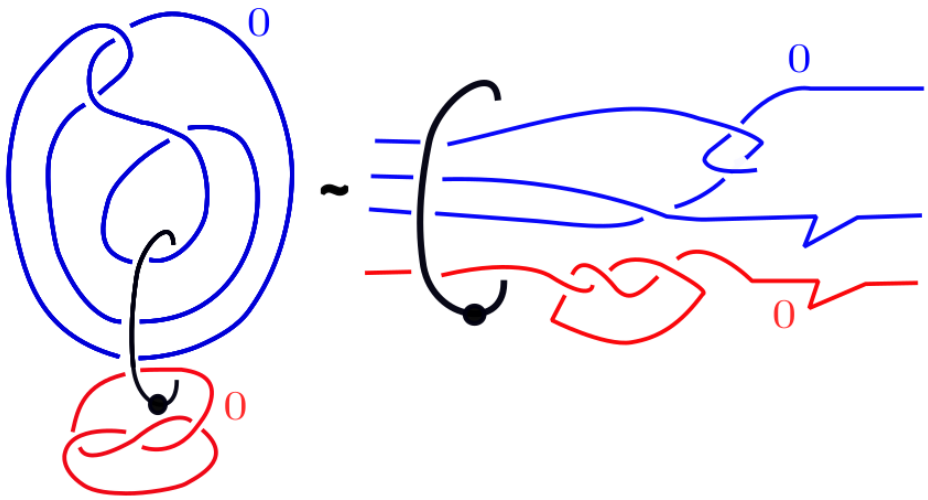

Figure 11.9: Description of X with additional cusps.

inequality yields $\frac{1}{2}(2+2) + 0 \leq 2g(\Sigma) + 2 \implies g(\Sigma) \geq 2$. Thus there cannot be a genus 1 surface as in the case of X'. This completes the proof.

Remark 35 *In the next chapter, I will actually show that there is a genus* 2 *surface in* X *generating* $H_2(X)$.

Chapter 12

CONSTRUCTING SURFACES, DIAGRAM MANIPULATIONS, SOME COMPUTATIONS

In this last chapter, I will talk about constructing surfaces, and fill the gaps in the proof of the main result. In particular, I will be doing the following specifically:

- Computations of algebraic invariants,
- Different representation,
- Constructing surfaces,
- There exists $\Sigma_1 \hookrightarrow X'$ generating $H_2(X')$,
- There exists $\Sigma_2 \hookrightarrow X$ generating $H_2(X)$.

12.1 Computations of Algebraic Invariants

Let's first prove that Z is contractible. Looking at figure 11.2, we see that there is a single two handle and a single one handle. Recall that the fundamental group is generated by the 1-handles and 2-handles are giving the relations. In our case, $\pi_1(Z) \simeq \langle x|x\rangle \simeq 1$. Furthermore, recall that $C_k(Z)$ are generated by k-handles. In our case, the complex is as follows:

$$0 \to 0 \to \mathbb{Z} \to \mathbb{Z} \to \mathbb{Z} \to 0.$$

It can be seen that $H_*(Z) = H_*(B^4)$ as desired. Finally, combining Whitehead Theorem and Hurewicz's theorem, we see that it is indeed contractible. By symmetry, it can be seen that Z' is also contractible (or since they are diffeomorphic as stated before).

12.2 Different Representations

The descriptions as given in figure 11.8 is to be considered as braid closures and in that case they are not hard to figure out. In this section let's try to show that both X and X' are knot traces. Now, let's consider a diagram as depicted in figure 12.1. Note that, in this figure P can be anything and K is a single knot. The

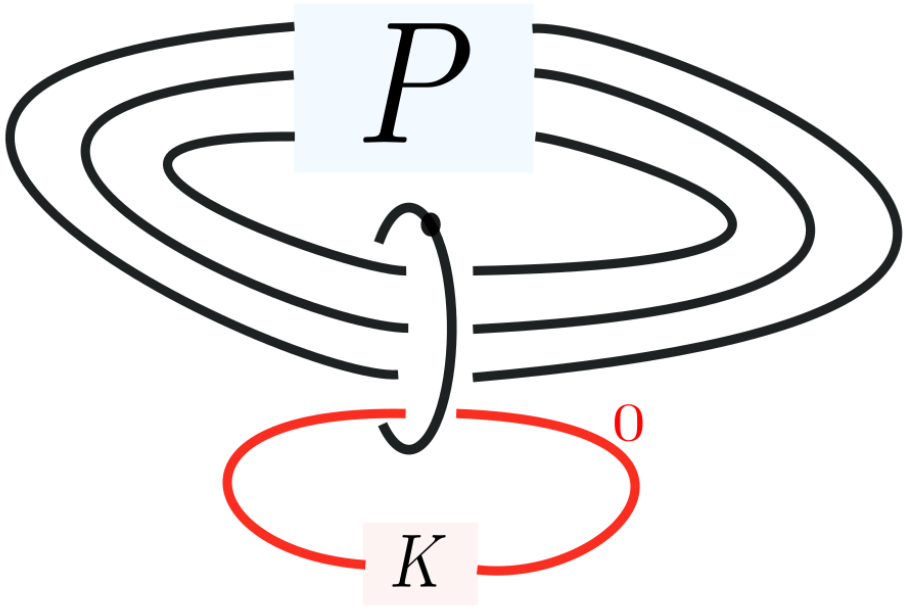

Figure 12.1: A cancellation trick.

goal is to cancel K and the one handle. A specific case of this is X. As depicted in this picture it is not possible to cancel them as there are other 2-handles going through the 1-handle. Thus, by sliding, we need to first make sure that all the other knots are not attached to the 1-handle. Consider 12.2. This way, we can slide the strands in order and since every strand will go around K, the resulting knot after the cancellation is as in figure 12.3.

In our case, the knot K is trefoil and one can draw the resulting knot and this

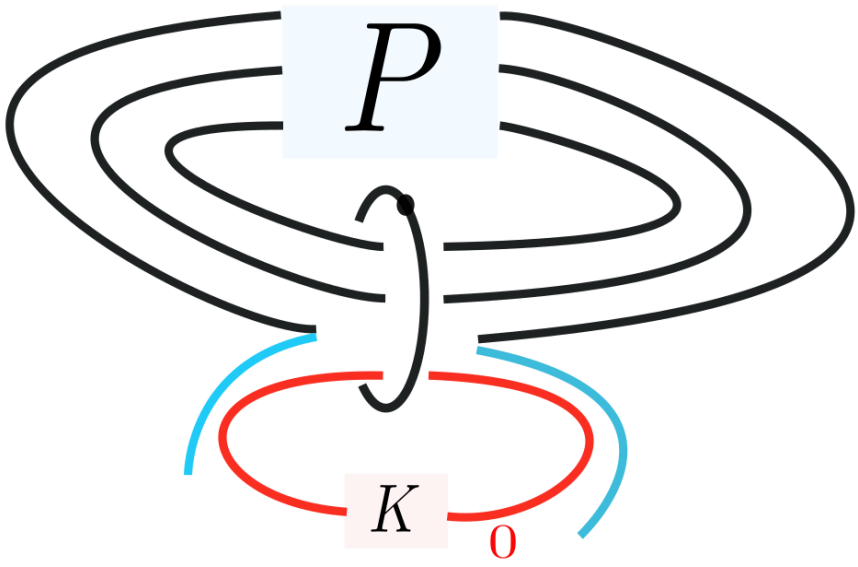

Figure 12.2: A cancellation trick, sliding part.

proves that X is a knot trace. For X', one can do it as follows: after getting rid of one of the cusps, one can pull the trefoil via the black strand and move it in between the one handle. Now, there is only one reason as to why we cannot cancel the 1-handle and the black 2-handle, which is the fact that the red 2-handle is attached to the 1-handle, but we can resolve this by sliding it through the black 2-handle. Now, we can cancel the black 2-handle and the 1-handle, the resulting knot is the modified red one. Thus, X' is a knot trace as desired.

12.3 Constructing Surfaces

In this short section, we will be talking about *Seifert* surfaces.

Definition 24 *A Seifert surface for an oriented link L in S^3 is a connected, compact, oriented surface contained in S^3 that has L as its oriented boundary.*

The easiest example is clearly the unknot, which bounds D^2. In fact, any embeddings

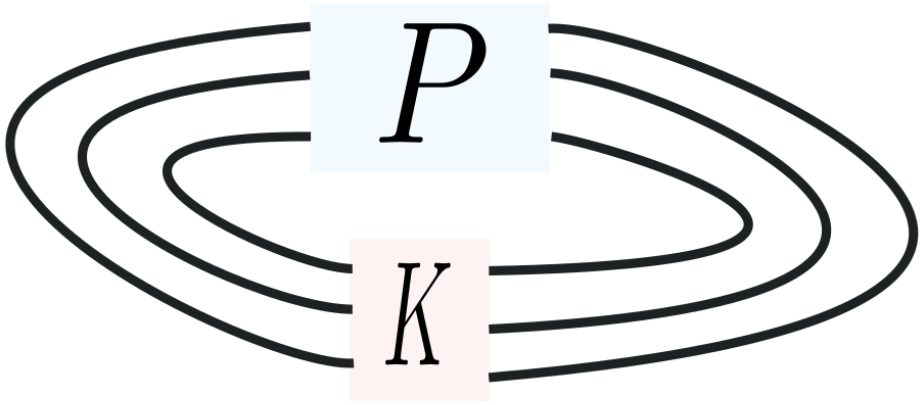

Figure 12.3: After the cancellation trick.

into S^3 of a compact, connected oriented surface with boundary gives us an example of a link having a Seifert surface. Furthermore, we have the following result:

Theorem 18 *Any oriented link in S^3 has a Seifert surface.*

Proof *Let D be an oriented diagram for the oriented link L, then by applying the moves depicted in figure 12.4, we modify D. This new diagram is almost like D itself except for neighborhoods of the crossings. This new diagram consists of oriented simple closed curves, thus each bounds D^2. Now, we join these discs via half-twisted strips at the crossings. This forms an oriented surface with L being the boundary as desired. If not connected, take the connected sum of each of these surfaces.*

In the next two sections we will actually construct these surfaces for two cases that arose in the previous chapter. For now, let's consider an example. Consider figure

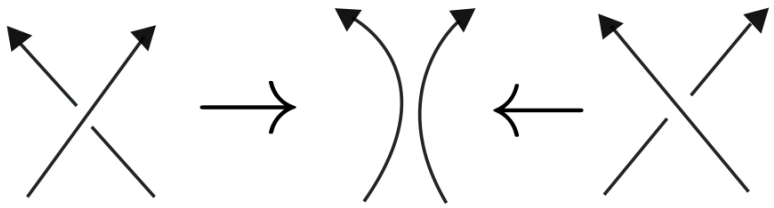

Figure 12.4: Seifert algorithm.

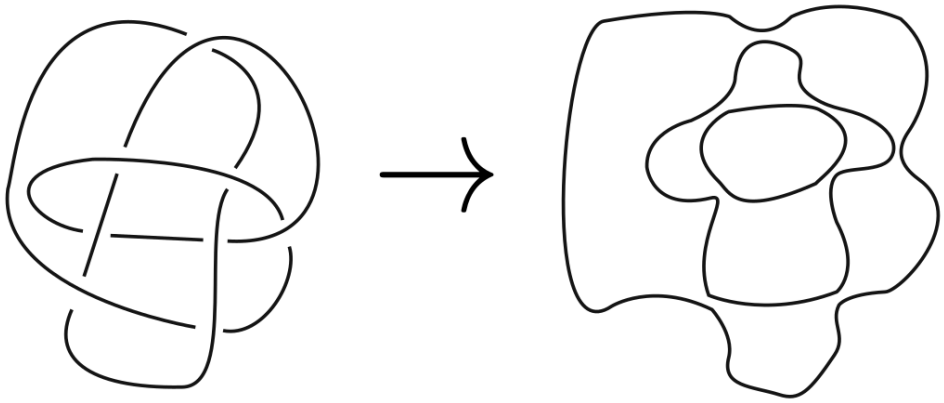

Figure 12.5: An example: Seifert algorithm.

12.5. The Seifert surface is then given by considering three discs at different altitudes and then adding eight half-twisted strips near the crossings to join the discs. Now, I would like to introduce a different way of looking at this procedure. We can think of this process as building a surface, at time $t = 0$, there is nothing, and we can add bands one-by-one, once we reach an unknot we can cap it off by a disc, at $t = 1$ we complete the construction. One can also simply just keep track of the number

of bands, boundary components and discs to compute the Euler characteristic and hence the surface. Let's do this for the trefoil knot. Consider figure 12.6. Here, on

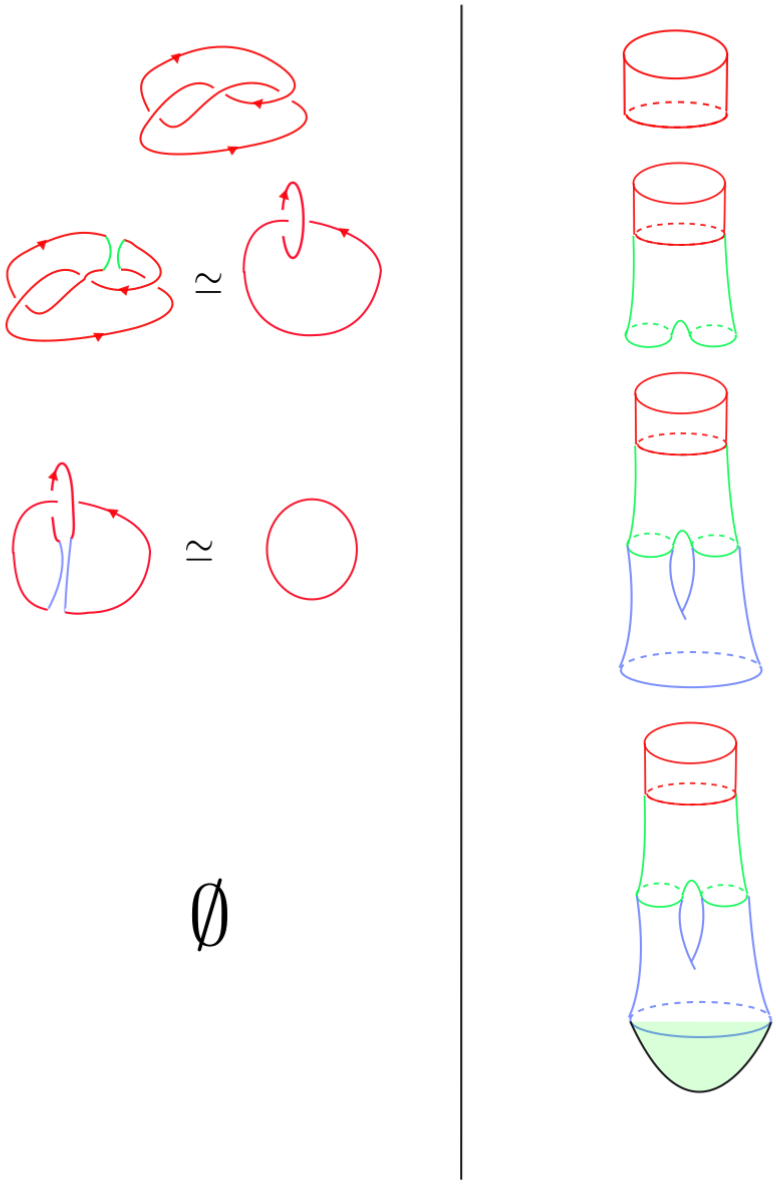

Figure 12.6: Constructing a Seifert surface for the trefoil knot.

the right, we are constructing the surface, for simplicity, on the right-hand side, the

cylinder in the first row denotes the trefoil. Actually, its top denotes the trefoil and then we start constructing the surface. In the second row, we add the first band, which introduces an arc in the surface and increases the boundary components (from one to two) as can be seen by looking at either sides of the figure. We add one more band and obtain the figure in the penultimate row, which again introduces an arc and together with the previous arc, we have a torus-like shape. We also end up with a single unknot, we cap it off by a disc and obtain the last picture, which is a torus with a boundary component. Thus, the trefoil knot bounds the torus with one boundary component. As mentioned before, we can also just keep track of the bands, discs and boundary components. In our link (it is just a knot) we have one component so the number of boundary components is just 1. We used a single disc and two bands. Thus (considering the closed surface after capping off the boundary component as well) $\chi = 0 - 2 + 2 = 0$, since for oriented surface $\chi = 2 - 2g$, where g denotes the genus of the surface, in this case $g = 1$, and we indeed have a torus.

12.4 Existence of $\Sigma_1 \hookrightarrow X'$ Generating $H_2(X')$

We almost already did this in the previous section, but let me just include some details here. Looking at any of the descriptions of X', one can easily see that the second homology is generated by the red 2-handle (because its signed intersection with the 1-handle is zero and it is the kernel). Therefore, as we already did, it gives us the torus (with one boundary component).

12.5 Existence of $\Sigma_2 \hookrightarrow X$ Generating $H_2(X)$

It was already proven that there cannot be a surface of genus one smoothly embedded in X that generates the second homology (via the adjunction inequality). But we claimed that there is a genus two surface generating the second homology of X. Let's first try to figure out a generator for the second homology of X. Consider figure 11.4 of X. Let α be the blue simple closed curve and β be the red one. Let h be the 1-handle portion of the diagram. Then, the boundary maps are, for, instance $\partial\alpha = \partial\beta = h$ depending on the orientations. Thus, $H_2(X) \simeq \langle \alpha - \beta \rangle$. We will now

show that $\alpha - \beta$ bounds a surface of genus 2 with two boundary components (α and β). Let's take a look at figure 12.7. In this figure, we stopped at the point where

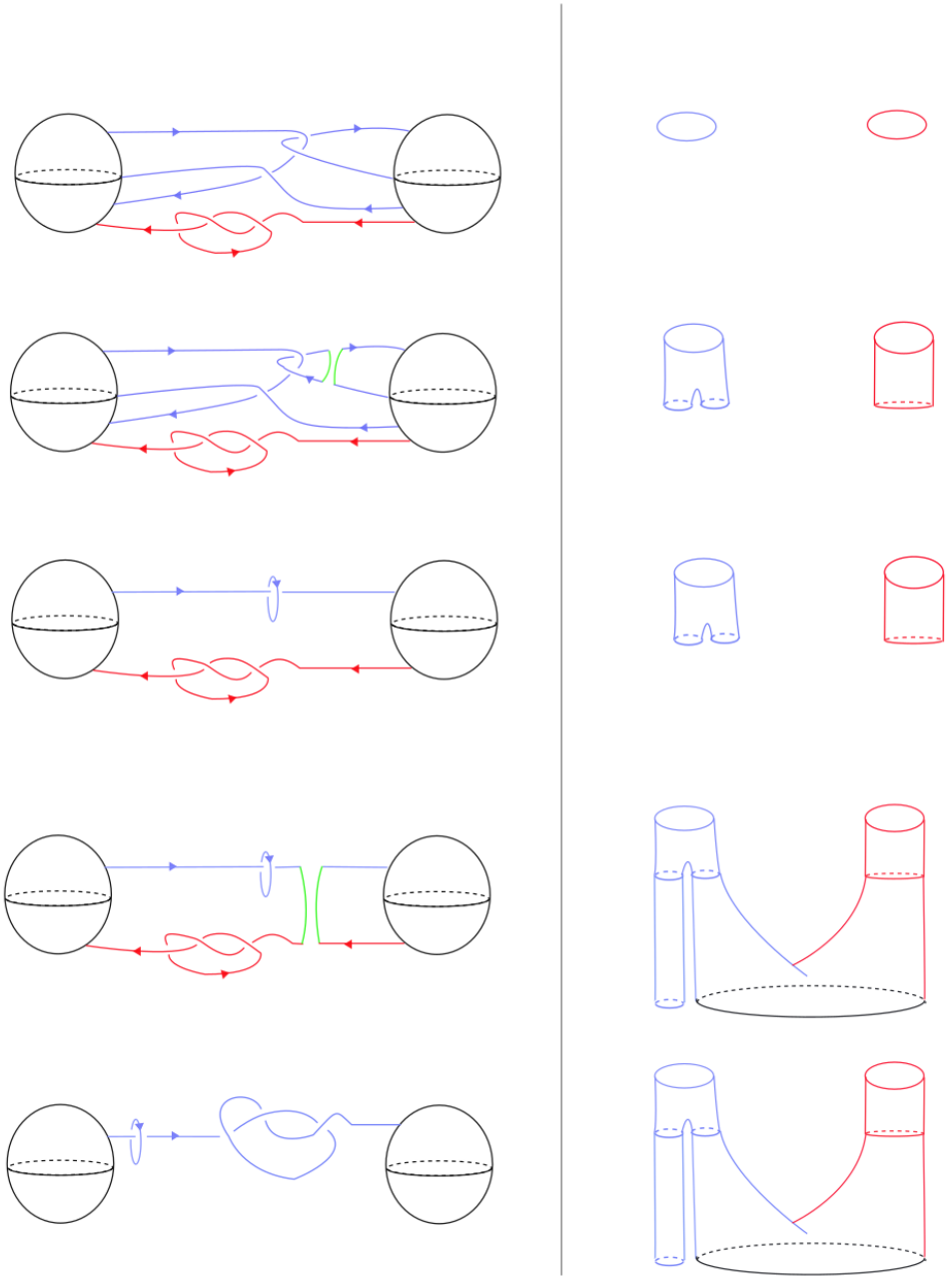

Figure 12.7: Constructing a Seifert surface for $\alpha - \beta$, first part.

we have a trefoil and an unknot attached to it. The trefoil part is now denoted by the black circle and it will bound a surface of genus 1, combining it with the other piece, we will have a surface of genus 2 as desired. One can follow the rest of the

steps described above in figures 12.8 and 12.9.

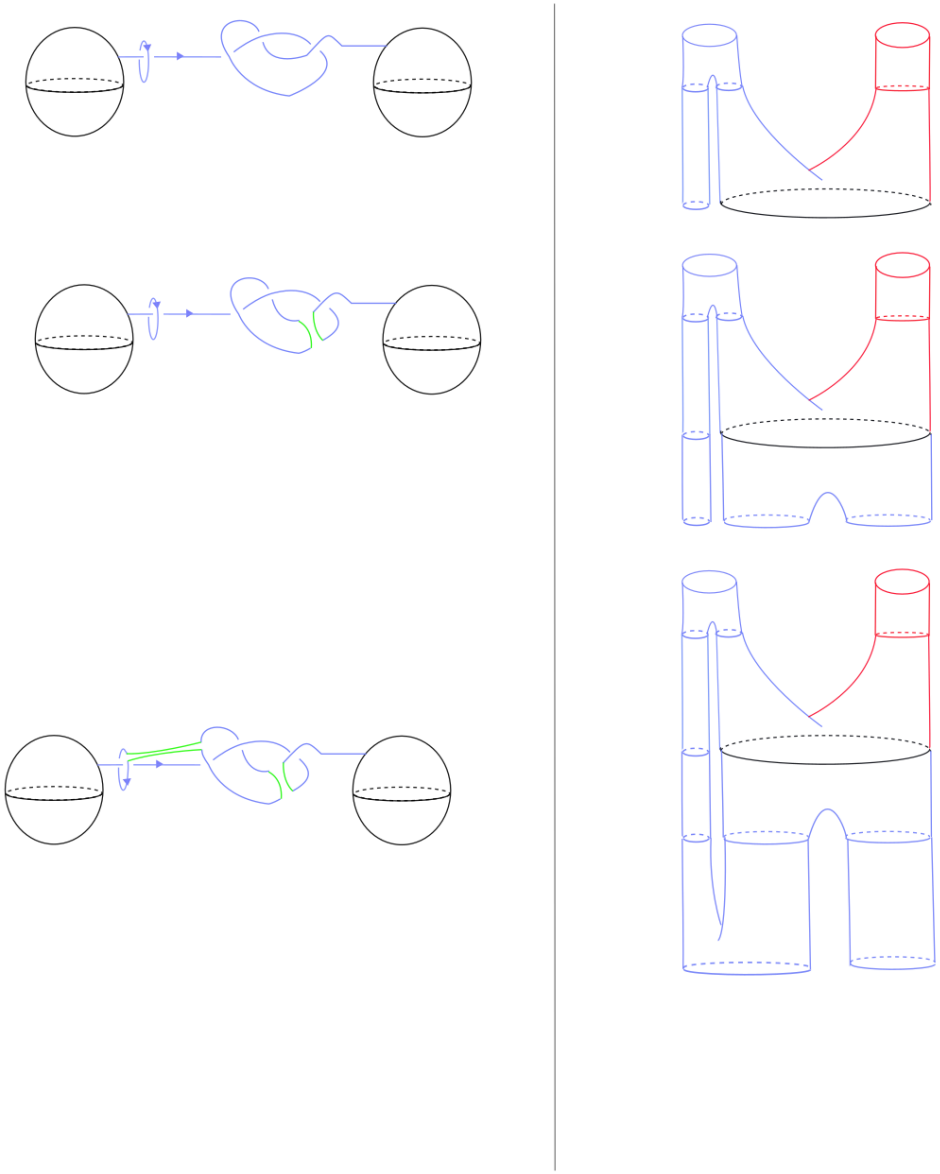

Figure 12.8: Constructing a Seifert surface for $\alpha - \beta$, second part.

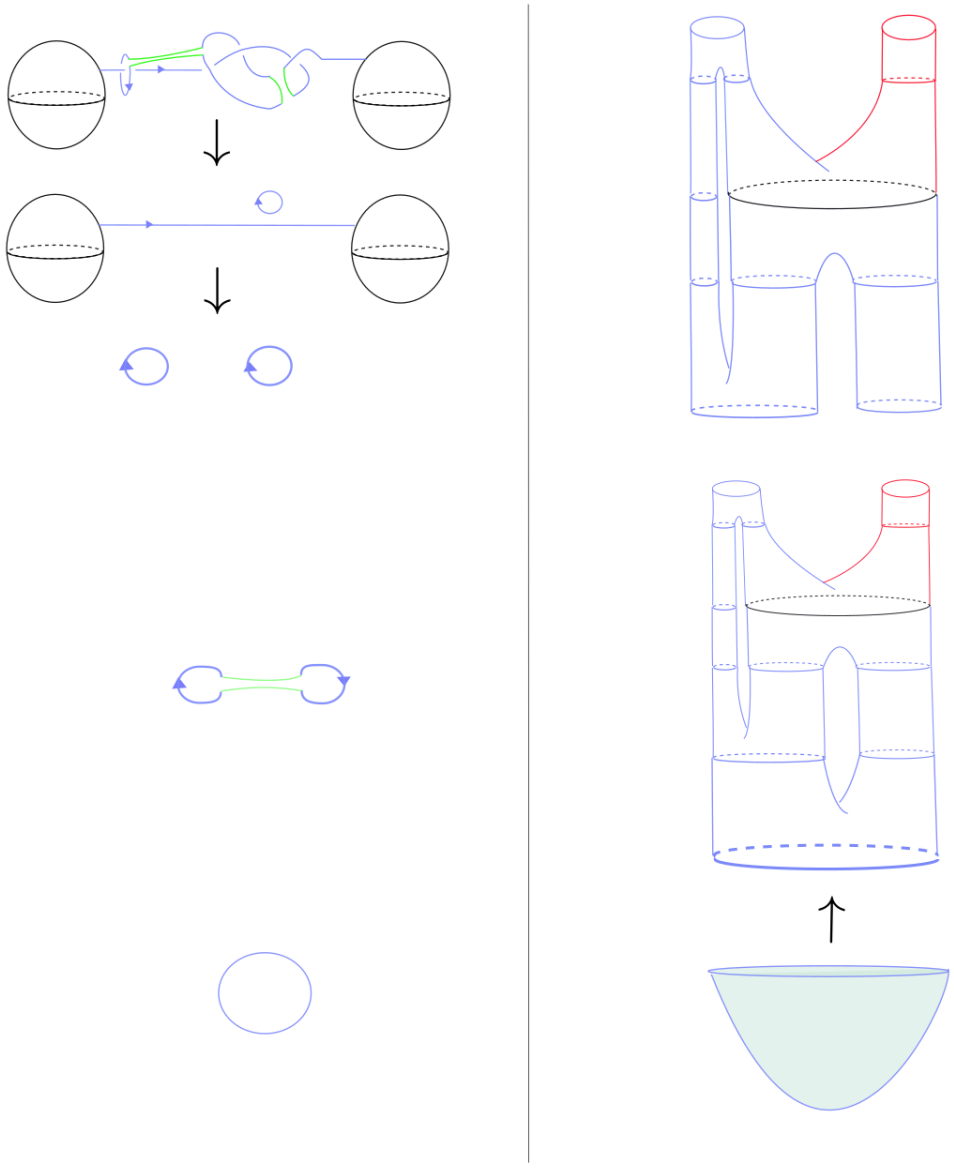

Figure 12.9: Constructing a Seifert surface for $\alpha - \beta$, third part.

BIBLIOGRAPHY

[1] Akbulut, S. An exotic 4-manifold. *J. Diff. Geom. 33* (1991), 357–361.

[2] Akbulut, S. 4-*Manifolds*. Oxford University Press, 2016.

[3] Akbulut, S., and Matveyev, R. Exotic structures and adjunction inequality. *Turkish Journal of Mathemaics 21*, 1 (1997), 47–53.

[4] Audin, M., and Damian, M. *Morse Theory and Floer Homology*. Springer, 2014.

[5] Freedman, M. H., and Taylor, L. A universal smoothing of four-space. *J. Diff. Geom. 24* (1986), 69–78.

[6] Gompf, R. E. An infinite set of exotics $\mathbb{R}^4$'s. *J. Diff. Geom. 21*, 283-300 (1985).

[7] Gompf, R. E. Handlebody construction of stein surfaces. *Annals of Mathematics 148* (1998), 619–693.

[8] Gompf, R. E., and Stipsicz, A. *4-Manifolds and Kirby Calculus*. American Mathematical Society, 1999.

[9] Laudenbach, F., and Poenaru, V. A note on 4-dimensional handlebodies. *Bull. Soc. Math. France 100*, 337-347 (1972).

[10] Lee, J. M. *Introduction to Smooth Manifolds*. Springer, 2003.

[11] Matsumuto, Y. H., and Saito, M. *An Introduction to Morse Theory*. American Mathematical Society, 2002.

[12] Milnor, J. W. On manifolds homeomorphic to the 7-sphere. *Annals of Mathematics 64*, 2 (1956), 399–405.

[13] Milnor, J. W. *Lectures on the H-cobordism Theorem*. Princeton University Press, 1965.

[14] Milnor, J. W. *Morse Theory*. Princeton University Press, 1969.

[15] Özbağci, B., and Stipsicz, A. *Surgery on Contact 3-Manifolds and Stein Surfaces*. Springer, 2004.

[16] Prasolov, V., and Sossinsky, A. *Knots, Links, Braids and 3-manifolds*. American Mathematical Society, 1997.

[17] Stallings, J. R. The piecewise-linear structure of euclidean space. *Proceedings of the Cambridge Philosophical Society 58* (1962), 481–488.

[18] Stang, R. Simply-connected 4-manifolds with a given boundary. *Topology Appl. 52*, 2 (1993), 161–167.

[19] Taubes, C. H. Gauge theory on asymptotically periodic 4-manifolds. *J. Diff. Geom. 25* (1987), 363–430.